

H.I.

AC LOSSES IN TYPE II SUPERCONDUCTORS

Frank DiSalvo

AMP 206
Contract No. NAS 8 - 5279
September 1966

supported by
GEORGE C. MARSHALL SPACE FLIGHT CENTER
NATIONAL AERONAUTICS AND SPACE ADMINISTRATION
Huntsville, Alabama

and

AVCO CORPORATION

GPO PRICE \$ _____

CFSTI PRICE(S) \$ _____

Hard copy (HC) 3.00

Microfiche (MF) .65

ff 653 July 65

N68-19140

(ACCESSION NUMBER) _____ (THRU) _____

49

(PAGES) _____ (CODE) _____

CR-61654

(NASA CR OR TMX OR AD NUMBER) _____ (CATEGORY) _____

FACILITY FORM 602



EVERETT RESEARCH LABORATORY

A DIVISION OF AVCO CORPORATION

AC LOSSES IN TYPE II SUPERCONDUCTORS

by

Frank DiSalvo

AVCO EVERETT RESEARCH LABORATORY
a division of
AVCO CORPORATION
Everett, Massachusetts

September 1966

Contract No. NAS 8-5279

supported by

GEORGE C. MARSHALL SPACE FLIGHT CENTER
NATIONAL AERONAUTICS AND SPACE ADMINISTRATION
Huntsville, Alabama

and

AVCO CORPORATION

ABSTRACT

Two experiments were set up to determine the AC losses in Type II superconductors, one using electrical methods and the other using calorimetric measurements. In the first experiment, alternating currents up to the quench current were applied to several feet of coiled Nb-Zr wire. The results, measured electrically, showed that: 1) the loss was directly proportional to the frequency (50-2000 Hz); 2) at currents below 4 A rms, the loss is proportional to I^2 ; 3) at currents above 6 A rms, the loss is proportional to $I^{3.7}$; 4) the magnitude of the loss depends sharply on the geometry of the wire configuration. The results of 4) lead to the conclusion that the magnetic field at the surface of the wire is the important variable in the determination of losses--not the transport current.

In the second experiment, an AC magnetic field was applied to the superconductor (Nb-Zr, Nb-Ti, Nb₃-Sn) and independently transport currents could be applied. The results, as measured calorimetrically, have shown with zero transport current: 1) the loss is linearly proportional to frequency $10 < f < 100$ Hz (the frequency range of the experiment); 2) the loss at fields below a certain value is proportional to $H^{3.4}$, at fields greater than that value the loss is approximately proportional to H (measured to $.6 \text{ Wb/m}^2$) this loss is shown to be hysteresis loss. If the conductor is stabilized², the sample will carry currents to the short sample characteristic. As the transport current increases, the losses increase slightly. The loss due to the transport current is shown to be proportional to I^2 .

Flux jumping, induced by the AC field, may be completely eliminated by reducing the wire diameter.

The loss observed both with and without transport current agree with the Bean model of superconductivity.⁶

PRECEDING PAGE BLANK NOT FILMED.

AC LOSSES IN TYPE II SUPERCONDUCTORS

Introduction

Superconductivity exists only below a temperature characteristic of the material which is called the critical temperature (T_c). The superconductivity of the material may be destroyed by applying either a large enough DC magnetic field or a large enough DC current density, these are called the critical field (H_c) and the critical current density (J_c) respectively. These three factors, temperature, magnetic field, and current, interact when more than one is present. The interaction is such that if more than one factor is present, the transition from a superconducting to normal metal occurs at values lower than the critical values measured individually. The exact relationship between the variables necessary to cause this transition is a complicated function which depends upon the material and its metallurgical history. Typical values for Type II superconductors are:

$$T_c \sim 10 - 20^\circ\text{K}, \quad H_c \sim 5 - 20 \text{ wb/m}^2$$

and

$$J_c \sim 10^{10} \text{ amp/m}^2$$

When the material is superconducting, DC currents can pass through it without loss; that is, the electric field is zero everywhere inside and $E \cdot J = 0$. For short samples (several inches long) in liquid He (4.2°K), the plot of the current density necessary to cause the superconducting to normal transition at different magnetic fields is called the short sample characteristic. However, if long lengths are tested with poor thermal contact to the coolant, the transition (called quench) current falls far short of that predicted by the short sample characteristic¹. This is called the coil effect. Recently, the coil effect has been "circumvented" by stabilization of the superconductor². If alternating fields or currents, however, are applied to even short samples of superconductors, losses result. This article is concerned with the various phenomena which contribute to these losses.

A. Losses Due to Applied AC Transport Currents

Samples were made from approximately two meter lengths of Nb-Zr 10 mil diameter wire. They were immersed in liquid He at 4.2°K and the loss was measured when AC currents were applied (frequency: 50 Hz to 2000 Hz). The loss was calculated by measuring the voltage across the

sample (V_s), the current through it (I_s), and the phase angle between V_s and I_s . (The system is shown and discussed in Appendix A.) The sample current could be varied from zero to the quench value at any particular frequency. (The quench value is that current at which the conductor suddenly exhibits its normal resistivity.) Under AC conditions there is a power loss in the sample - thus the temperature of the sample increases. Also, under AC conditions, instabilities such as flux jumps are more likely to occur. For these reasons the quench current can be less than predicted by the DC short sample characteristic.

The results are shown in Figs. 1 and 2. Figure 1 shows that the loss at constant transport current, I_s , is linearly proportional to frequency. This result supports a hysteresis loss mechanism, where the loss is the energy represented by the area enclosed in the "quasi-static" hysteresis loop multiplied by the frequency. Figure 2 shows that the loss at constant frequency is proportional to I_s^n where $n \approx 2$ for $I_s < 4$ A rms and $n = 3.7$ for $I_s > 4$ A rms. This change in slope has been observed by others.³ When the currents are small (less than 4 A-rms) they flow only on the surface. However, at higher currents the current flows through a large portion of the conductor cross section and obviously a more complicated situation exists.

To show that the $I_s^{3.7}$ loss is not due to the slight temperature increase in the conductor, a sample was potted in epoxy to reduce the thermal conductivity to the surrounding liquid helium. At the same power input, the temperature of the sample would be higher than that of the sample unpotted. Figure 3 shows the results as compared to the same sample unpotted. The losses are the same within error except at currents very close to the quench current, where an appreciable increase in temperature has caused an increase in the losses. Thus at currents up to about the critical current, the loss is proportional to $I_s \sim 3.7$ and is not a temperature effect.

Many authors^{3,4} have found the loss proportional to I_s^n , $3 < n < 4$, but the magnitude of the losses varied considerably. The type of sample used, however, also varied - there were straight sections,³ Bifilar coils^{4,5} and solenoids. To determine the effect of geometry upon the loss, the same sample was wound in several different ways and the losses measured. The results (Fig. 4) show that the loss at the same frequency and current is a strong function of geometry. The losses observed in the bifilar coil agrees with the data of others who have measured losses in bifilar coils.^{4,5} The only electromagnetic variable that had been changed was the magnetic field (H) produced by the currents. Because of the geometry, the "opposing coil" has larger fields at the surface of the wire; also, larger losses are observed. Since $H = gI$ where g is a geometry function, the loss may purely be due to H . The peak magnetic fields produced in the samples are about 0.2 Wb/m^2 . This explains the large "disagreement" in the magnitude of the losses observed by many authors.^{3,4} It is due to the difference in the geometry of their samples.

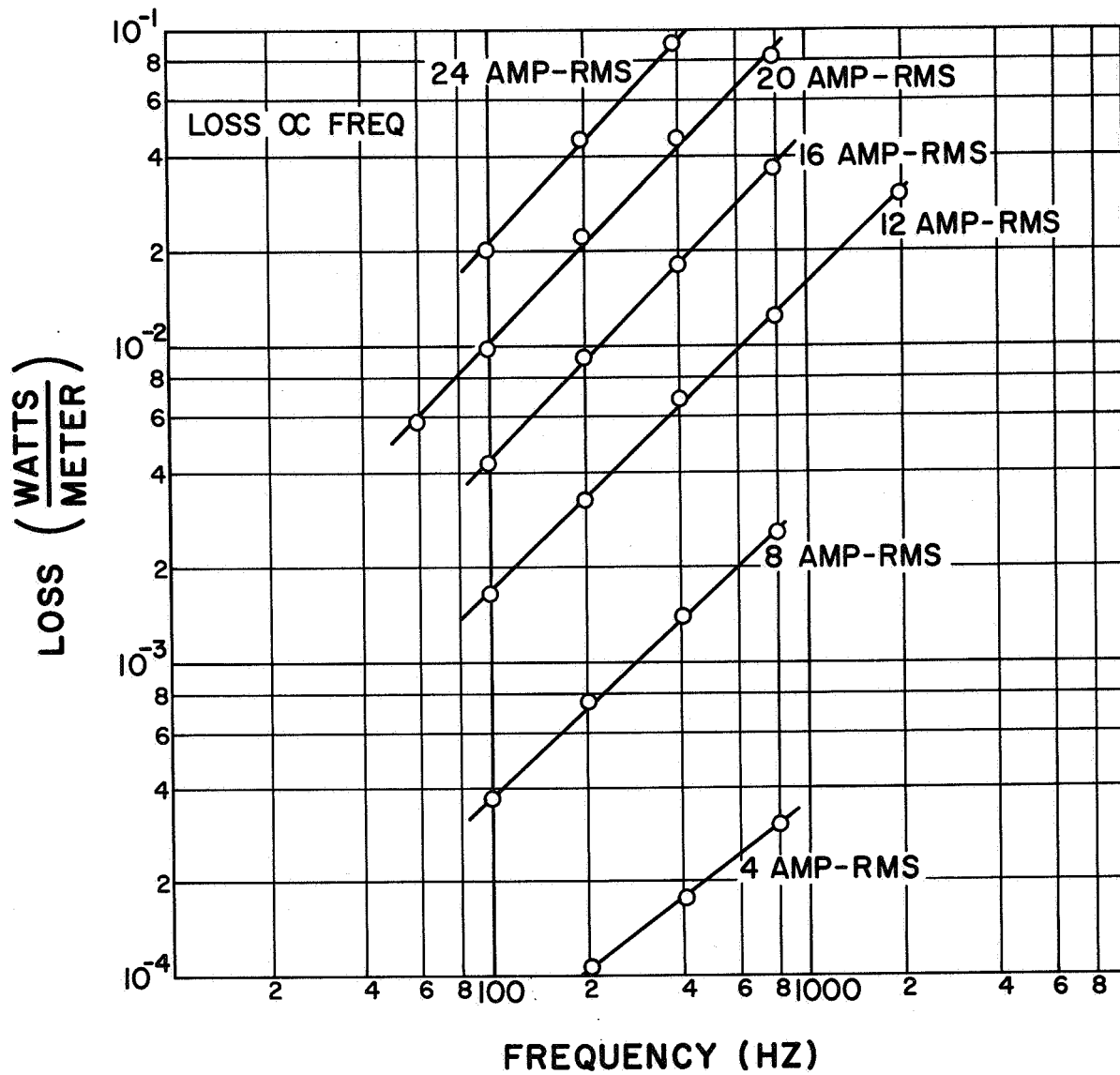


Fig. 1 Loss vs Frequency at Constant Sample Current

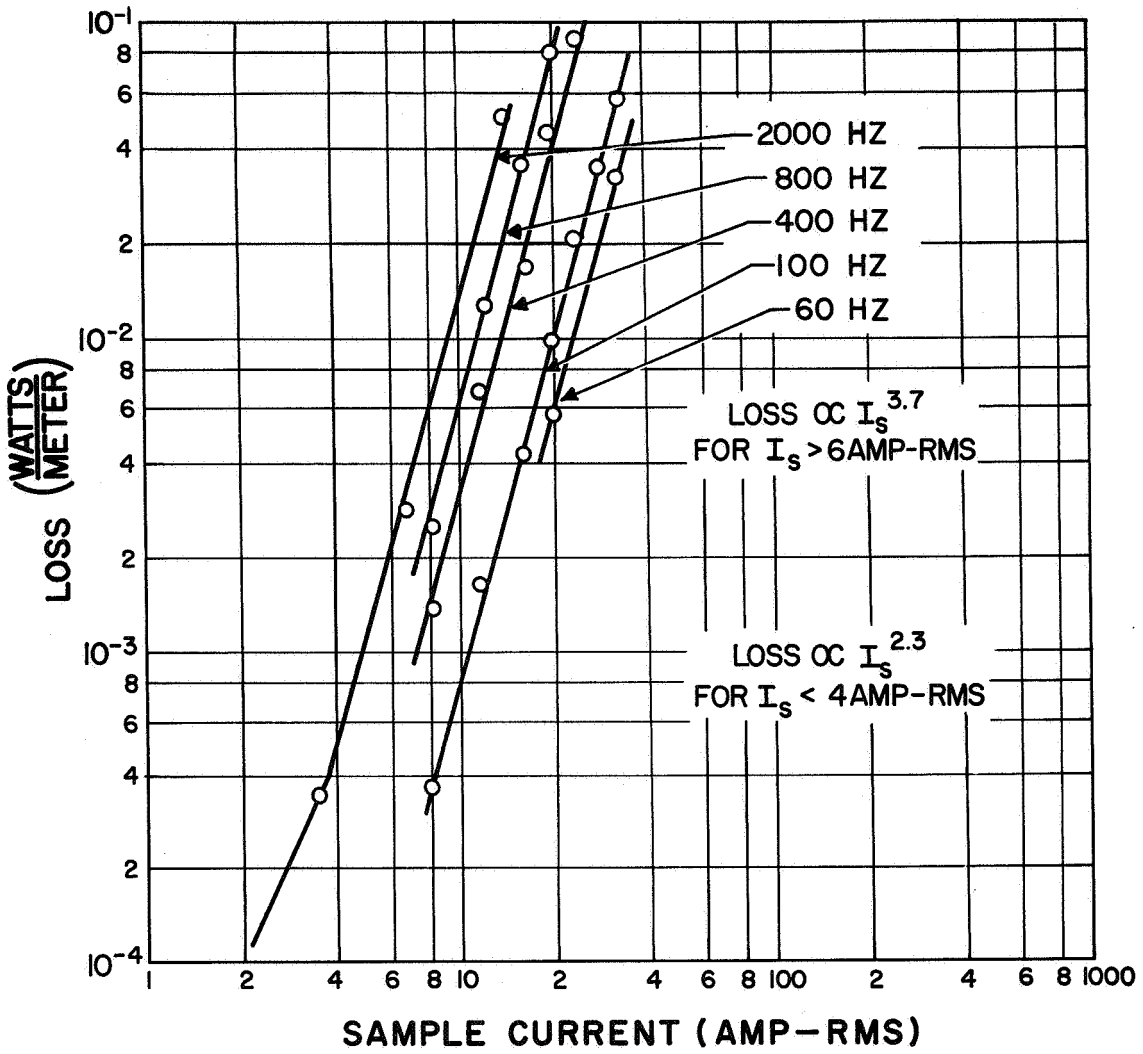


Fig. 2 Loss vs Sample Current at Constant Frequency

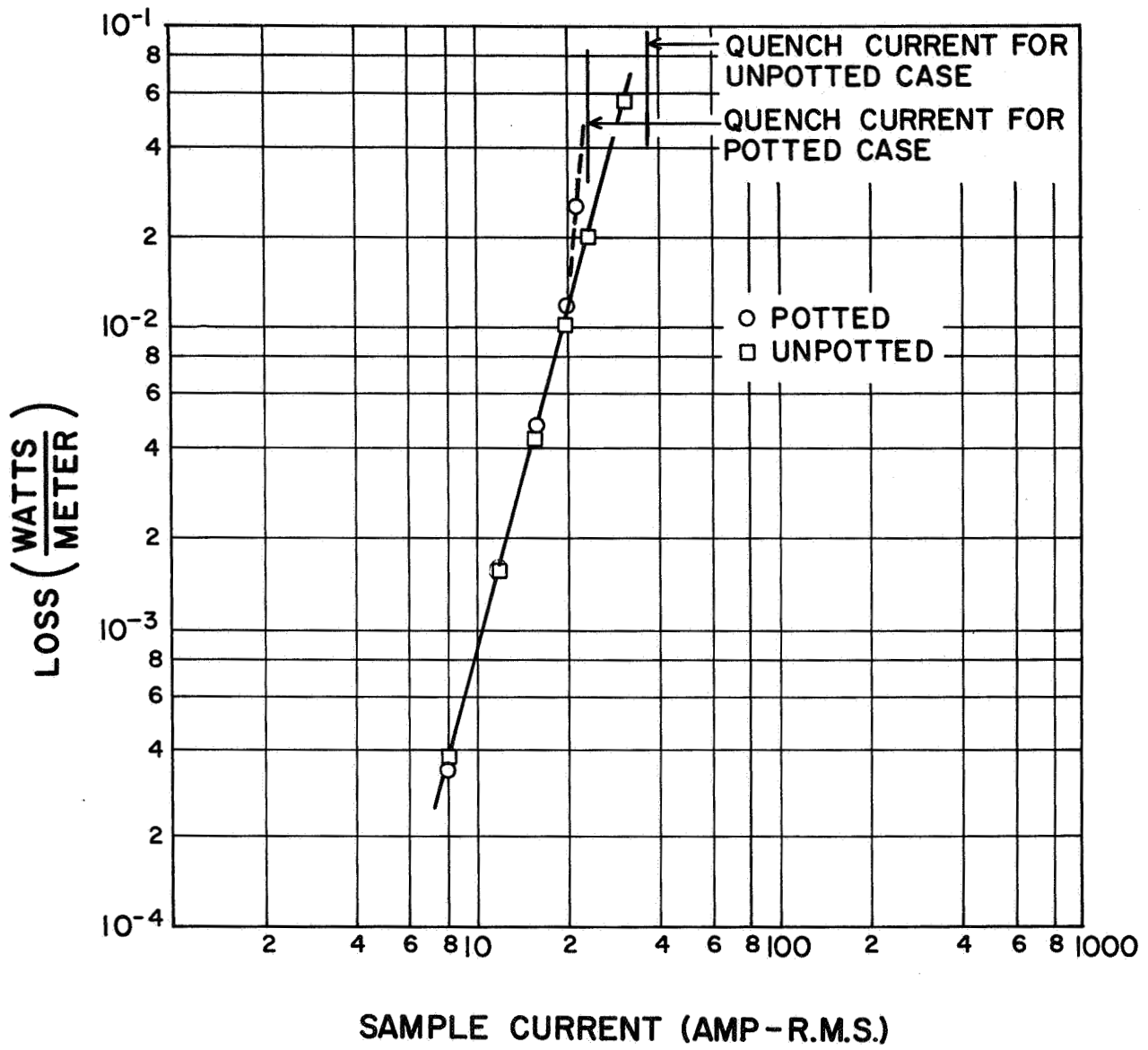


Fig. 3 Loss vs Sample Current at 100 Hz

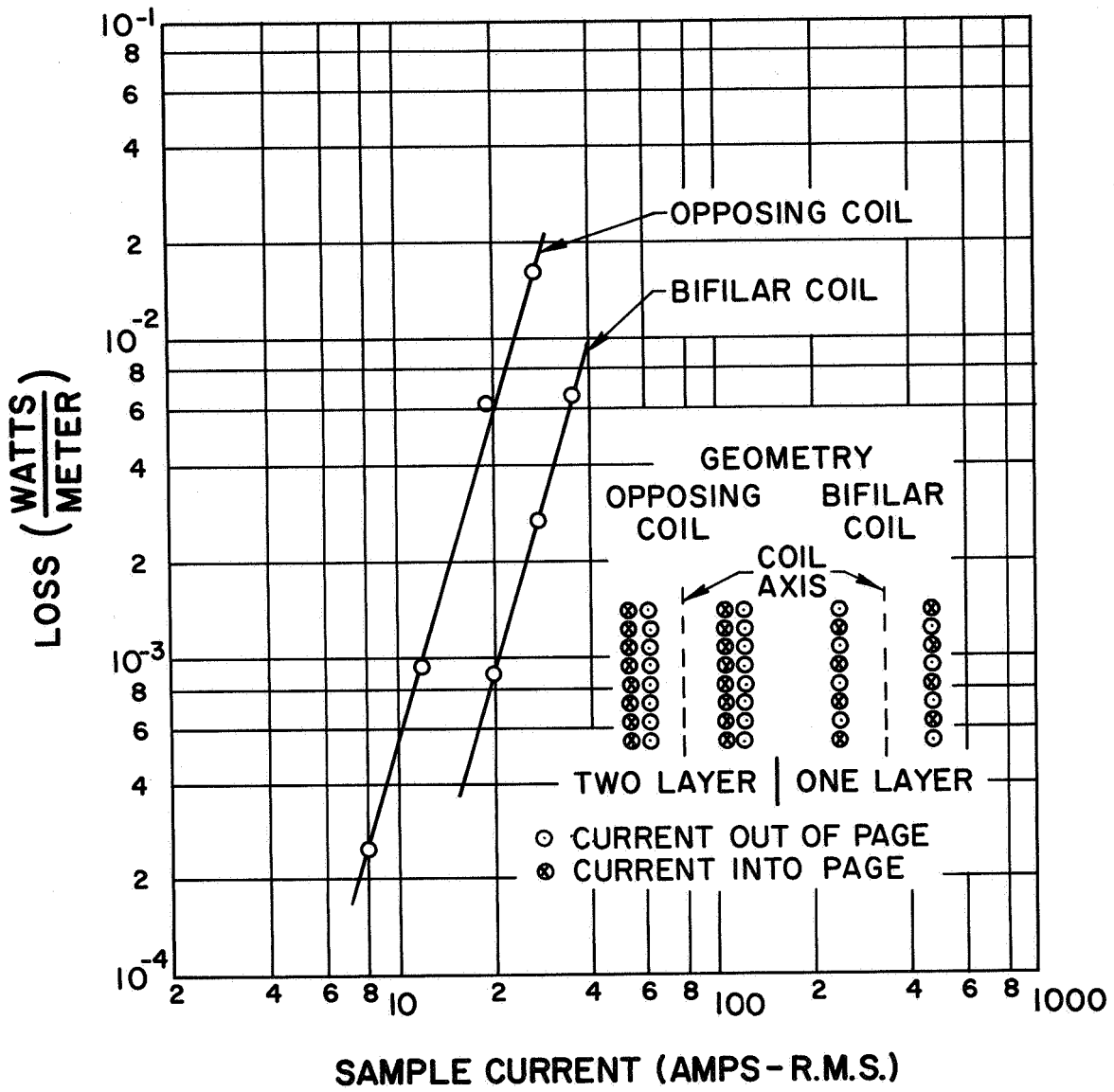


Fig. 4

Loss vs Sample Current at 100 Hz

B. Losses Due to Externally Applied Fields

A second experiment was designed so that the magnetic field could be controlled over the surface of the wire and transport currents could be independently applied.² To do this a magnet was designed to produce magnetic fields up to 0.6 Wb/m^2 in the gap at frequencies from 5 to 100 Hz. The losses were calculated by measuring the boil-off of helium gas from the sample. (See Appendix B for drawings and discussion of the apparatus.) Samples were made from 5 and 10 mil diameter Nb-Zr wire, 2.5 and 5 mil diameter Nb-Ti wire, and strips of various widths of GE and RCA Nb₃Sn. Sample lengths were from 10" to 20".

The results for a typical sample of Nb-Zr are shown in Figs. 5 and 6. Figure 5 shows that at constant peak applied field the loss increases linearly with frequency. Figure 6 plots the loss per cycle per meter length of the sample vs the peak applied field. These losses occur without any transport current in the wire. They are due entirely to the externally applied magnetic field and may be identified as a hysteresis loss. Figure 7 shows some of the experimental magnetization curves that were observed in the experiment for the sample. The measured loss was equal to the loss calculated from the enclosed area to within 10%. * A point is included at 4 Wb/m^2 which is a calculated loss. This loss was calculated from a magnetization curve of 10 mil Nb-Zr wire with no heat treatment. This point falls almost exactly on the extrapolated loss curve. These results are typical of Nb-Zr, Nb-Ti and Nb₃Sn in that they show the same general characteristics. They agree fully with the Bean model of superconductivity and can be calculated directly from Maxwell's Equations.⁶ In Appendix C this model is explained in detail and its application to this experiment is discussed. Here, however, we shall only summarize these results and show some of the data obtained from experiment. According to this theory the current density in a sample, if it exists at all, must be critical in value and must penetrate in from an outside surface. Once established inside the sample they remain there indefinitely and can be changed only by means of an opposing critical current penetrating again from an outside surface. This gives rise to a hysteresis effect which results in the following dependence of losses on field and frequency:

- 1) The loss per unit surface area, L_A , is given by

$$\frac{C f H_o^3}{J_c} < L_A < C_1 f H_o^4, \quad H_o \leq H^*$$

- 2) The loss per unit volume, L_V , is given by

$$d f a J_c H_o < L_V < d_1 f a \ell n H_o, \quad H_o \gg H^*$$

*See Appendix B for a discussion of this measurement.

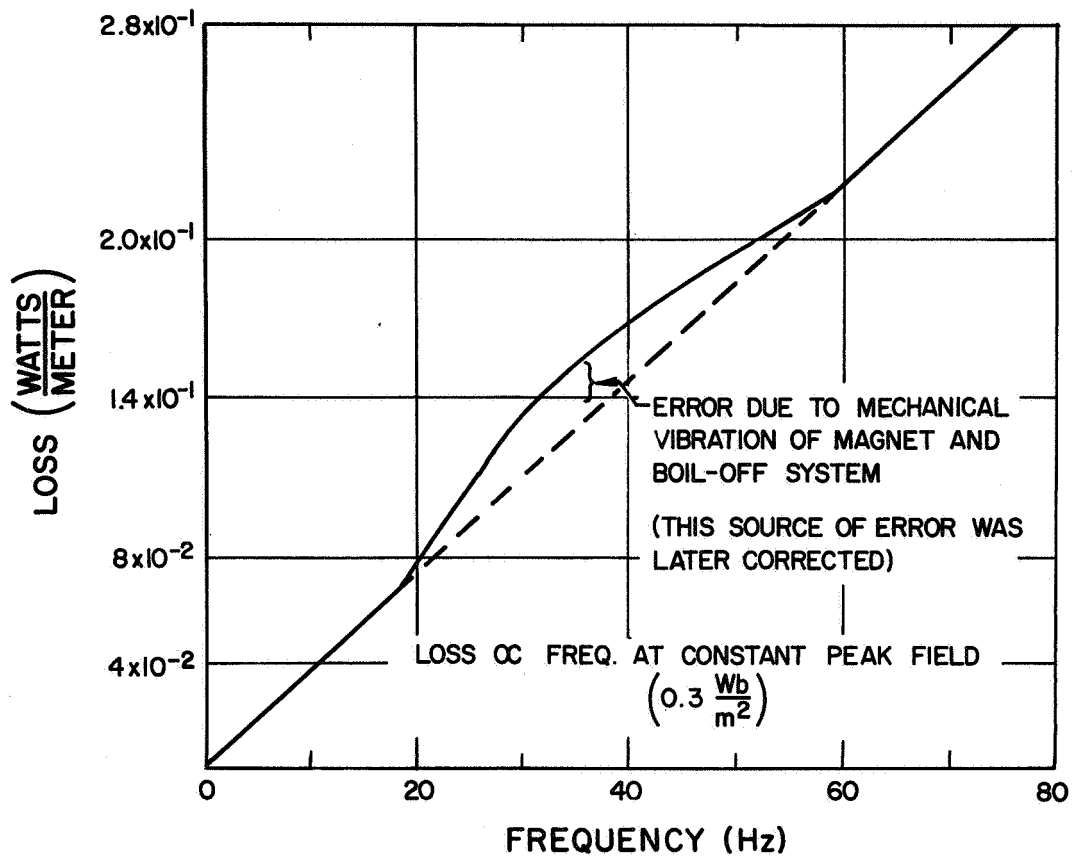


Fig. 5 Loss vs Frequency at Constant Peak Field

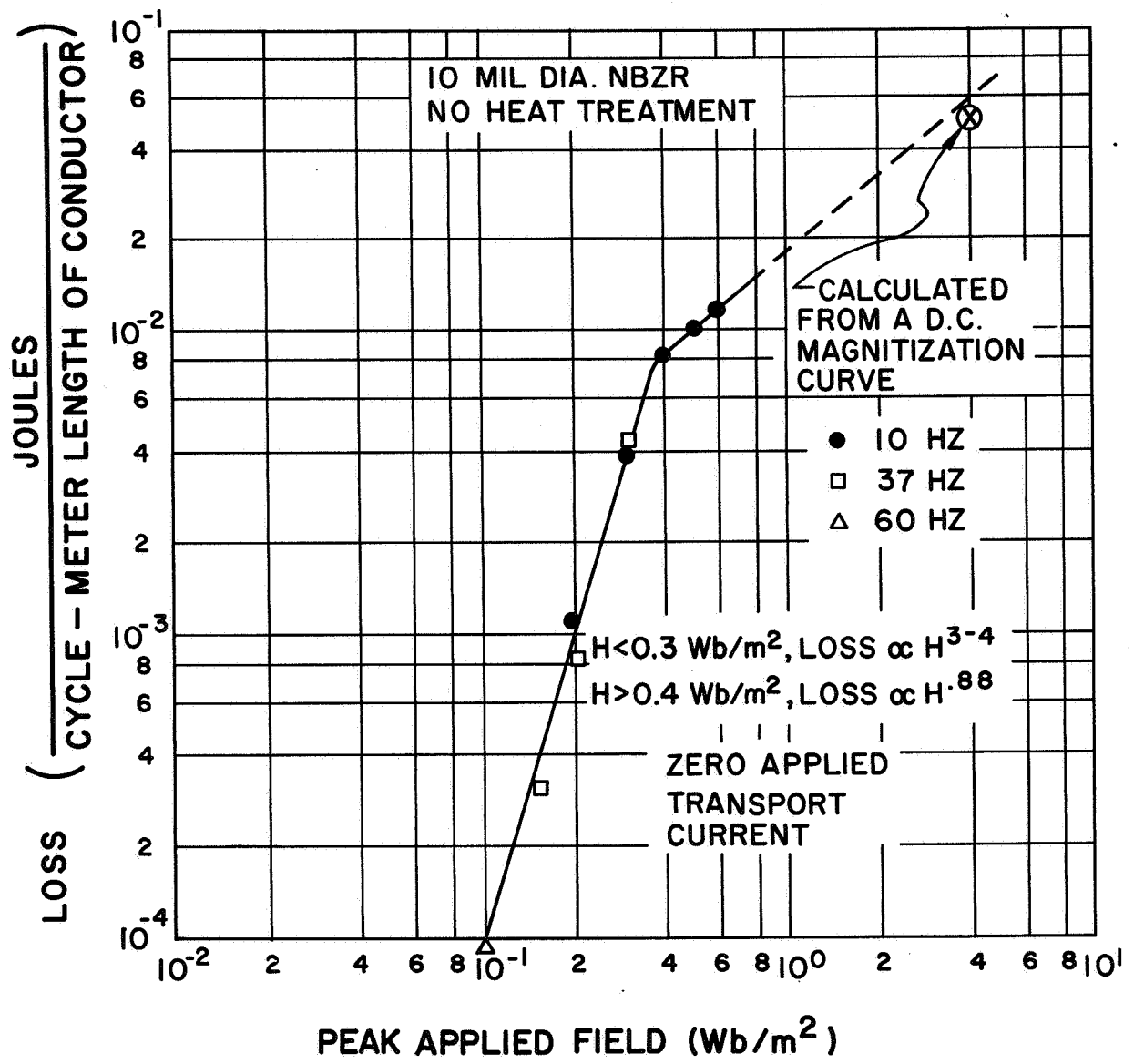
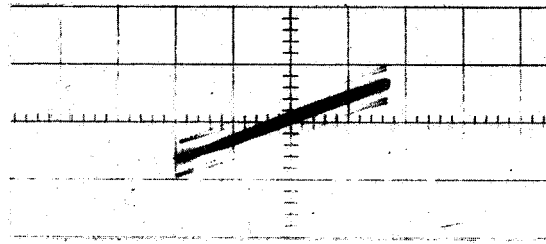
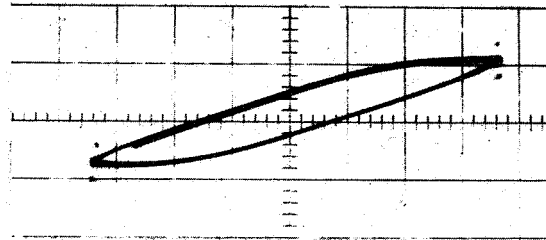


Fig. 6

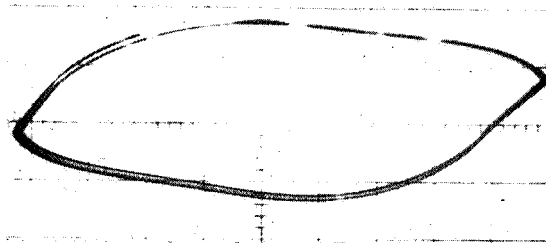
Loss vs Peak Applied Field



(1) PEAK APPLIED FIELD = 0.1 Wb/m^2



(2) PEAK APPLIED FIELD = 0.2 Wb/m^2



(3) PEAK APPLIED FIELD = 0.3 Wb/m^2

MAGNETIZATION (VERT. AXIS) VS
APPLIED FIELD (HORIZ. AXIS)

Fig. 7 Magnetization vs Applied Field

where $H^* = J_c a$

and f = frequency of applied magnetic field

H_0 = peak applied magnetic field

J_c = critical current density of the superconductor

a = half-thickness of sample

H^* = minimum magnetic field at which "shielding currents" are caused to flow over the whole volume of the superconductor

The constants, C , C_1 , d , d_1 , are somewhat different depending upon which model is used for the H-I characteristic, (e. g., the Bean or Kim models) and whether H_0 is greater than or less than H^* . Figure 8 shows loss per cycle per meter length of different superconducting wires. Each curve displays the transition of loss dependence from H_0^n , $3 < n < 4$, to approximately H_0 . The observed transition takes place rather rapidly both in Nb-Ti and Nb-Zr. In Nb-Zr the current density of the 10 mil diameter wire is approximately 0.6 that of the 5 mil diameter wire (measured ratios), thus when $H_0 < H^*$ the ratio of the losses at the same H_0 should be:

$$\frac{H_0^3/J_c (10 \text{ mil}) \cdot 2 \pi a_{10 \text{ mil}} \cdot \text{length}}{H_0^3/J_c (5 \text{ mil}) \cdot 2 \pi a_{5 \text{ mil}} \cdot \text{length}}$$

where $2\pi a$ = surface area of wire per unit length

$$\frac{J_c (5 \text{ mil})}{0.6 J_c (5 \text{ mil})} \times \frac{10}{5} = \frac{2}{0.6} = 3.3$$

The experimentally measured value is 3.2, as shown in Fig 8. The observed break point at H^* and the losses could be predicted by the theory to 10 or 15 percent in Nb-Ti and Nb-Zr. Note also the displayed dependence upon the radius when $H_0 > H^*$ in Nb-Ti (5 mil and 2.5 mil superconductor diameter). The ratio of the loss per cycle per meter at a particular H_0 is

approximately $8 \left(\frac{\text{Loss } 5 \text{ mil}}{\text{Loss } 2.5 \text{ mil}} \right)$. This is expected from theory:

$$\frac{\text{Joules}}{\text{Cm}^3 \cdot \text{Cycle}} = a a J_c H_0$$

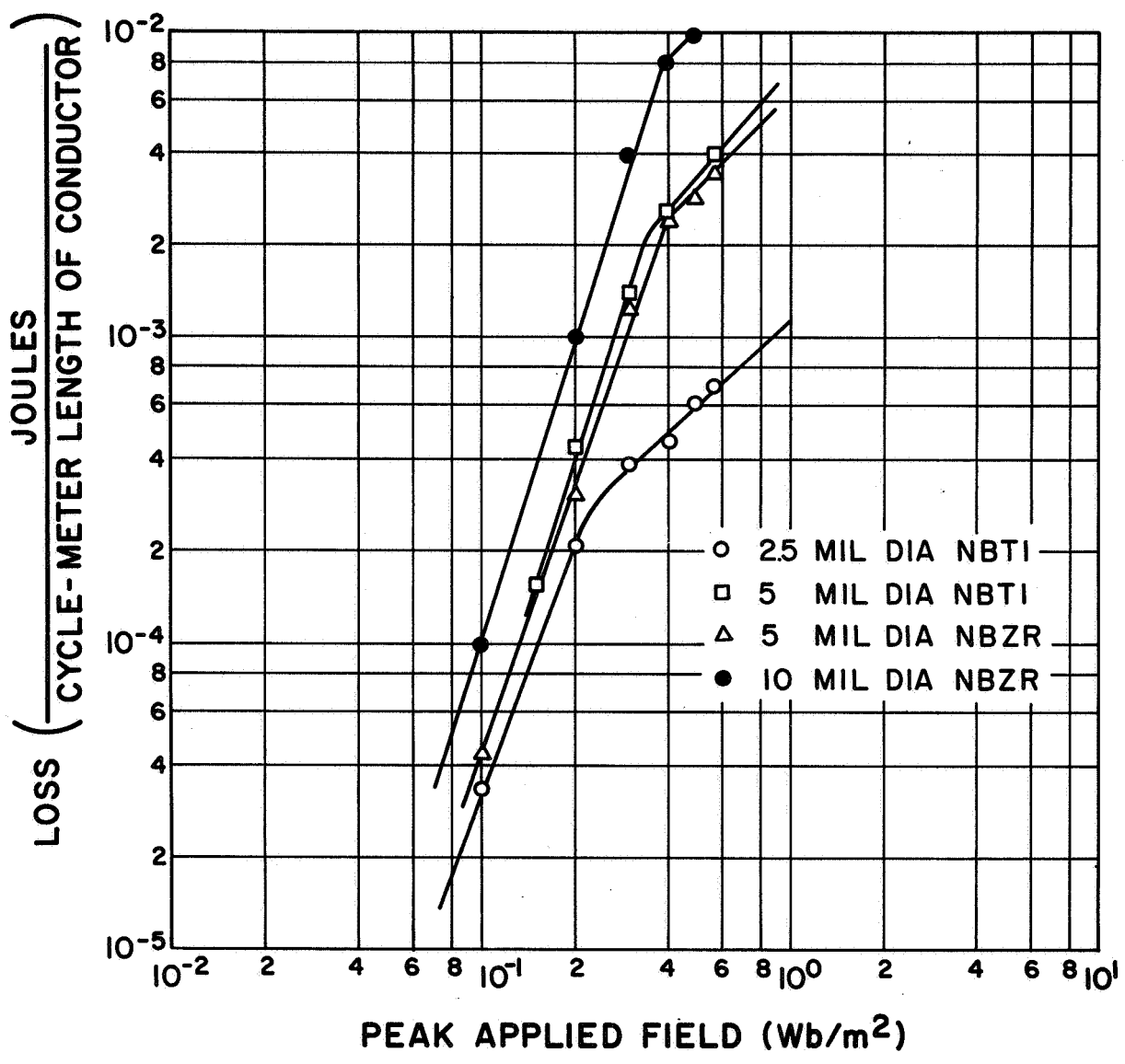


Fig. 8 Loss vs Peak Applied Field for Several Different Wires

$$\frac{\text{Joules}}{\text{meter} \cdot \text{cycle}} = \frac{\text{Joules}}{\text{Cm}^3 \cdot \text{Cycle}} \times (\text{vol. in cm}^3 \text{ per meter length of wire})$$

$$= \alpha \pi a J_c H_o \times a^2 \times 100 \text{ cm}$$

$$\frac{\text{Joules}}{\text{meter} \cdot \text{cycle}} = \alpha \pi a^3 J_c H_o \cdot 10^2$$

For Nb-Ti with the same heat treat J_c is approximately the same and at the same H_o , the ratio of the losses is:

$$\frac{\pi 10^2 J_c H_o (2.5)^3}{\pi 10^2 J_c H_o (1.25)^3} = (2)^3 = 8 \quad (\text{Nb-Ti})$$

The measured value is approximately 7.2 as shown in Fig 8. For the Nb-Zr wires, since J_c (10 mil Nb-Zr) \approx 0.6 J_c (5 mil Nb-Zr), the ratio of the losses when $H_o > H^*$ expected is:

$$\frac{0.6 J_c (5 \text{ mil}) (10)^3}{J_c (5 \text{ mil}) (5)^3} = 0.6 \times 8 = 4.8 \quad (\text{Nb-Zr})$$

The actual measured ratio is 4, as is shown in Fig. 8.

Measurements on Nb₃Sn conductors were harder to interpret. Both RCA and GE composite strips were used; and, in both cases, the loss was larger than initially expected. The loss data on the GE strip is complicated by the fact that there is a relatively large amount of Niobium present in the composite conductor. The data for the RCA conductor is shown in Fig. 9; also plotted is the initially expected loss according to the equation developed in Appendix C. The unexpectedly large losses in the RCA Nb₃Sn seems to be due to the fact that the Nb₃Sn is plated on a relatively thick substrate. An application of the method developed in Appendix C shows that the loss in the superconductor for the geometry used by RCA is given by:

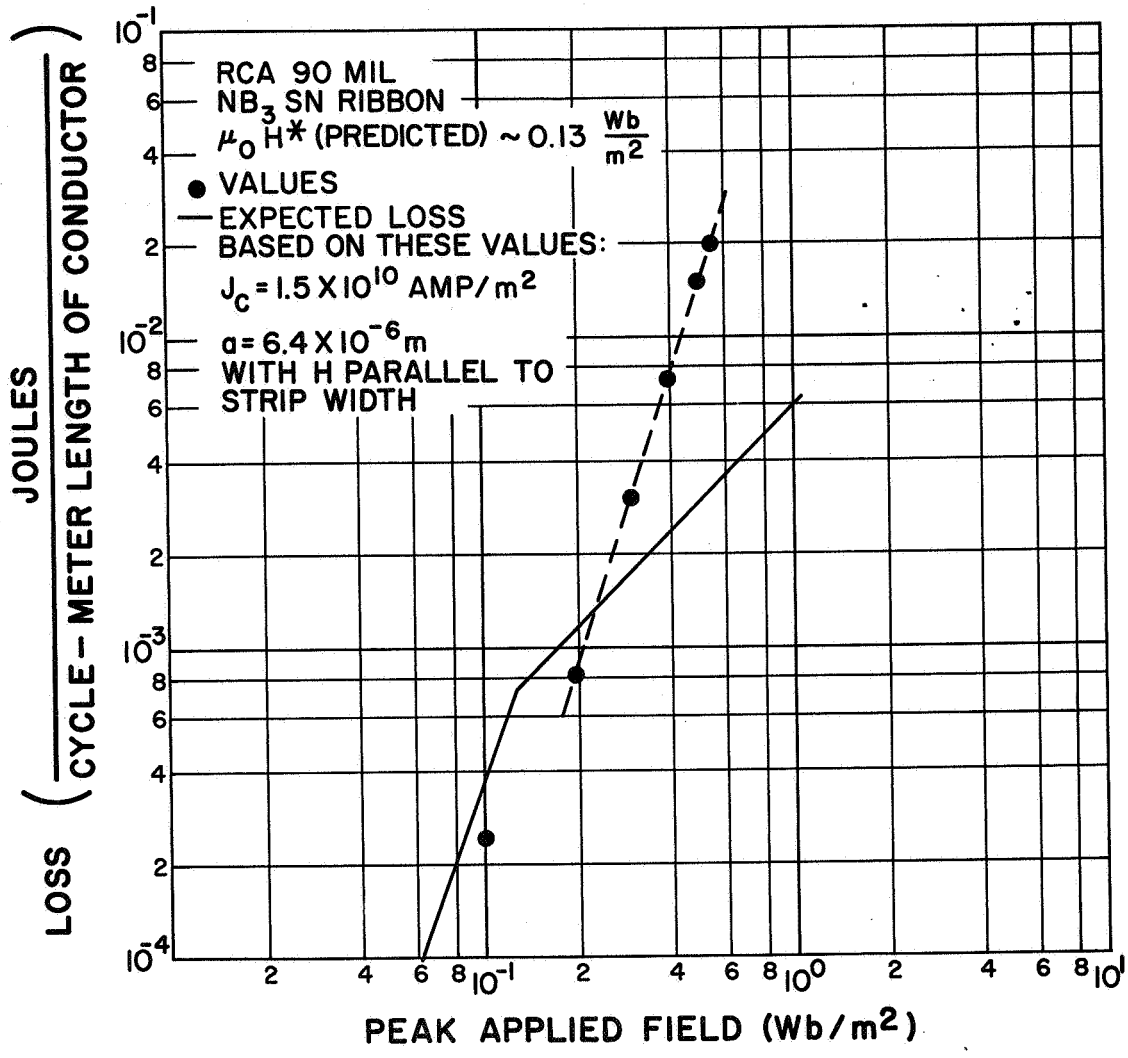


Fig. 9 Measured and Expected Loss vs Peak Applied Field for RCA Nb₃Sn Ribbon

$$\text{Loss} \left(\frac{\text{Joules}}{\text{Cycle} - \text{M}^3} \right) = 4 \mu_o J_c H_o d \quad H_o \gg H^*$$

where d = half-thickness of the substrate and $d \gg a$ (a being the half-thickness of the Nb_3Sn). The loss obtained for the same amount of Nb_3Sn without substrate is (see Appendix C)

$$\text{Loss} \left(\frac{\text{Joules}}{\text{Cycle} - \text{M}^3} \right) = 2 \mu_o J_c H_o a \quad H_o \gg H^*$$

The ratio of the actual loss to the "expected loss" is:

$$\text{RATIO} = \frac{2d}{a} > 1$$

Thus, the advantage of thin film superconductors in obtaining low losses is only obtained when the substrate is on the outside of the superconductor; that is, the center of the superconducting material must correspond to the geometrical center of the composite conductor. To be sure that the odd effects observed in the Nb_3Sn strip were not due to the overall rectangular cross-section of the conductor, losses were measured on an Nb-Zr strip. The strip (2 mils thick, 200 mils wide) losses were exactly as predicted and the curve "broke" slowly at the predicted H^* (see Fig. 10 for those results).

C. Interaction Between Transport Current and Applied AC Field

In some of the measurements taken in the work described above with the externally applied AC field the losses were observed to increase if a transport current near the critical value was also applied. This suggested a possible interaction between the AC applied field and the DC transport current. In order to explore this possibility a Bifilar sample was wound so that transport currents would have little effect on the axially applied AC field.

First, the effect of direct currents was investigated and we found:

1) Unless "stabilized," a superconductor will carry little current compared to its short sample critical current at the peak applied field. This is due to the large number of instabilities (flux jumps) that are produced by the AC magnetic field. Figure 11 shows the voltage across a Nb-Zr sample with $H_o = 0.4 \text{ Wb/m}^2 > H^*$, $f = 20 \text{ Hz}$ and a small transport current, I_s , to detect the flux jumps (the many "pulses" on the oscilloscope trace). Figure 12 shows the ratio of quench current to the DC short sample critical current at the peak applied field vs the peak applied field for several unstabilized Nb-Zr wires.

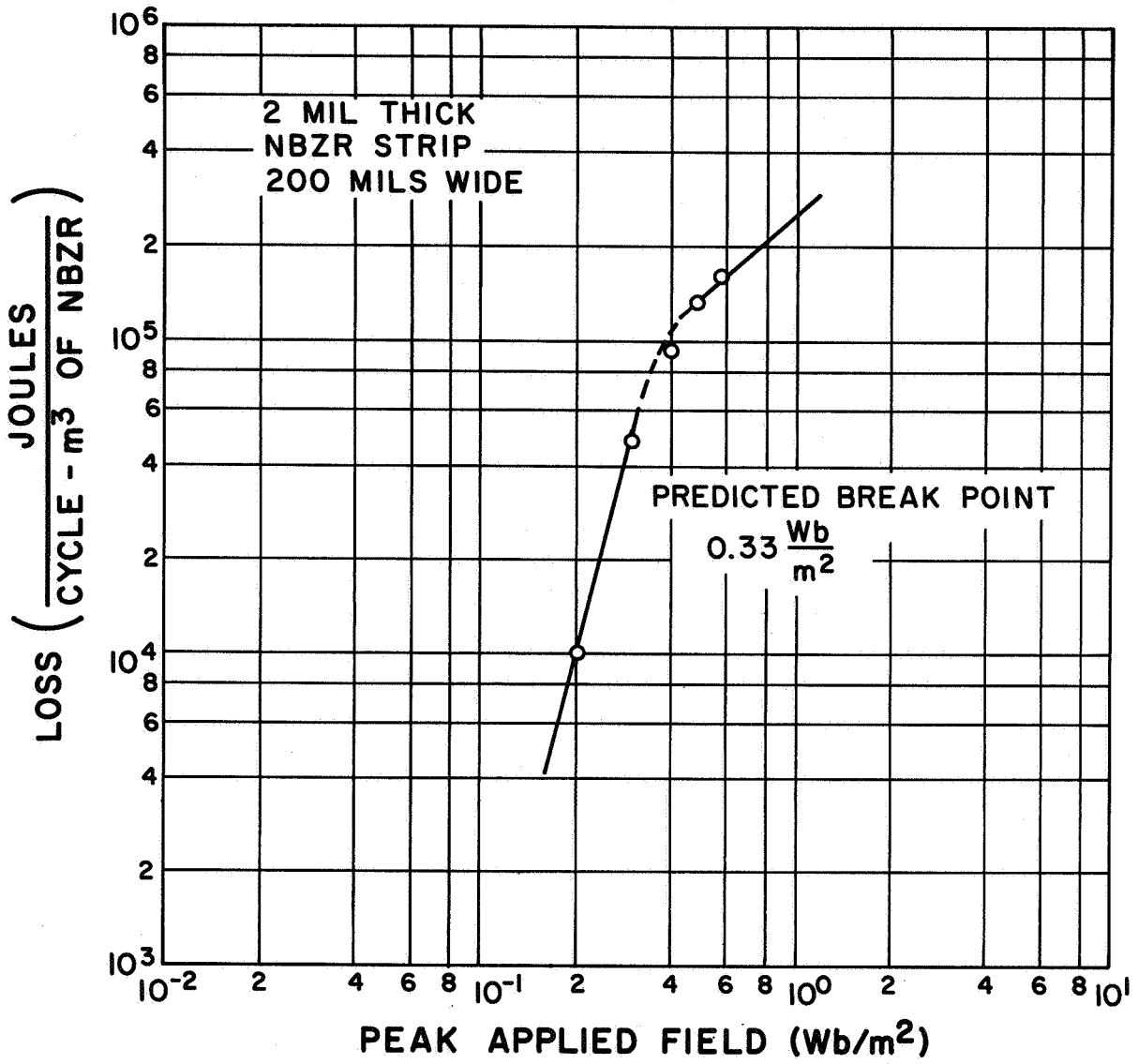
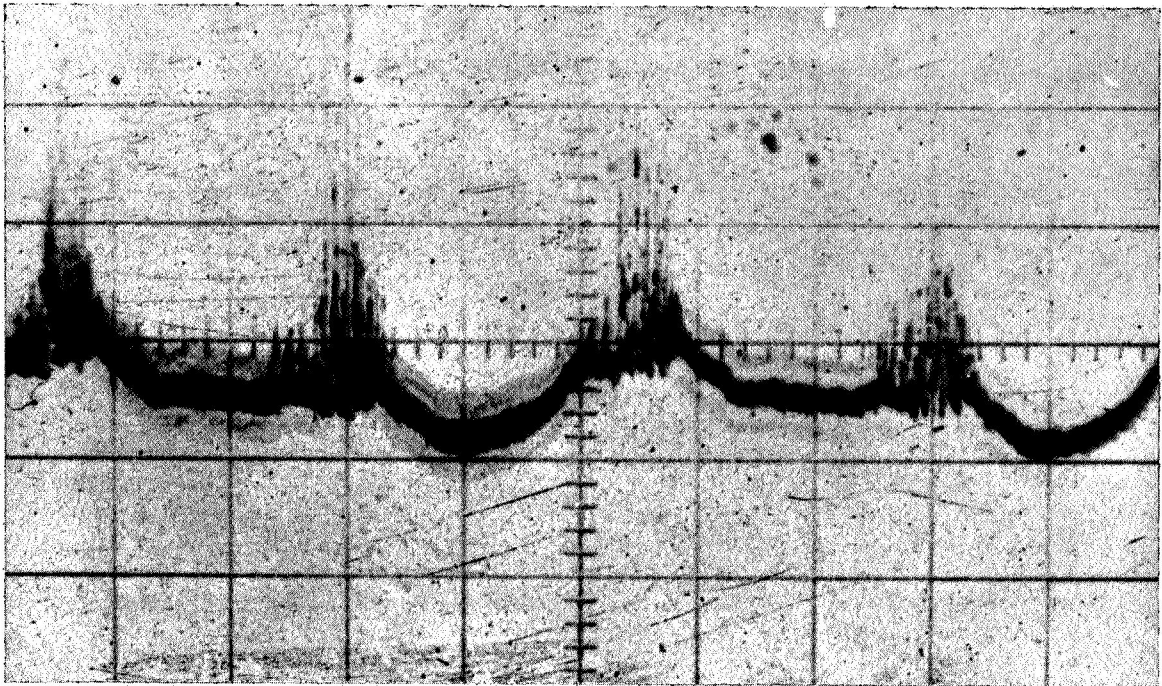


Fig. 10 Loss vs Peak Applied Field in Nb-Zr Strip



V_s (SAMPLE VOLTAGE) VS TIME
Y = 0.5 MV/CM
X = 10 MILLISEC/CM

COPPER COATED NBZR WIRE WITH SMALL TRANSPORT
CURRENT. THE SPIKES ARE FLUX JUMPS

Fig. 11 Flux Jumps in Nb-Zr Wire

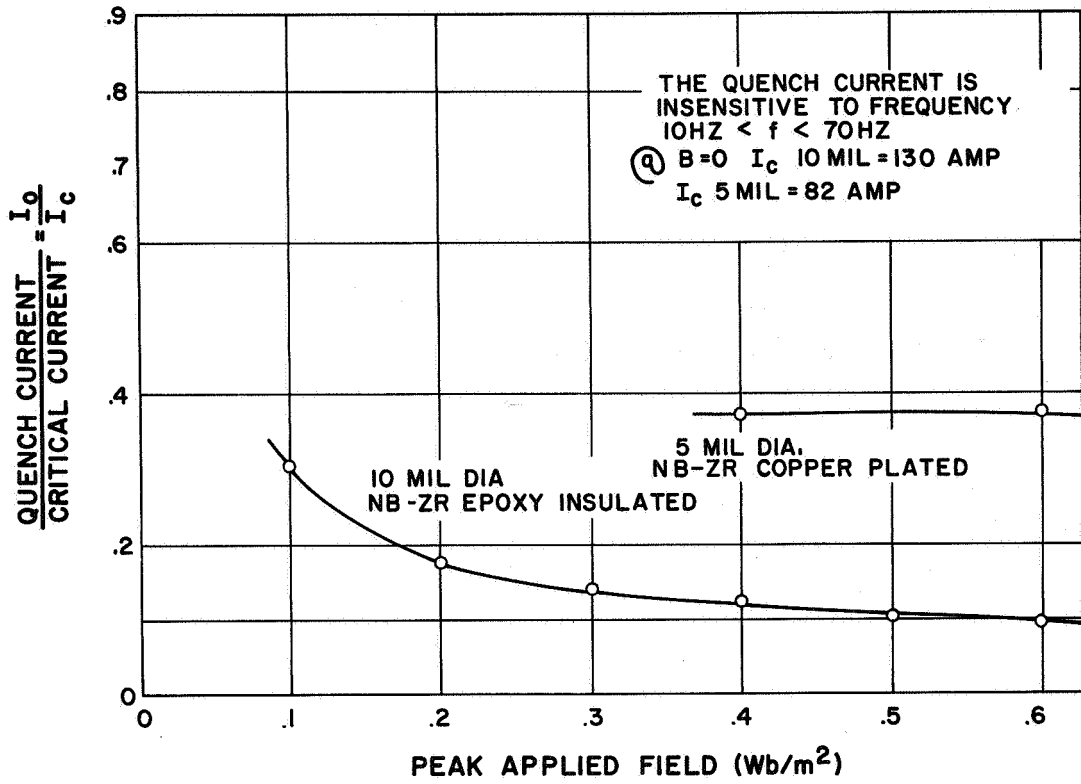


Fig. 12 Quench Current as a Function of Peak Applied Field

2) If the sample is stabilized as in the Avco technique, then currents up to the DC short sample characteristic may be carried. The losses increase as the short sample critical current, I_c , is approached. A typical example of this increase in stabilized Nb-Ti when $H_o > H^*$ is pictured in Fig. 13. The losses increase by approximately 60% when $I \approx I_c$ for stabilized conductors. This increase in loss is not due to flux jumps but due to the "flow resistivity" of the superconductor. The voltage across a Bifilar sample as a function of the applied field for several different transport currents (DC) is shown in Fig. 14. The applied field is: $H_o = 0.6 \text{ Wb/m}^2$ ($H^* \sim 0.5 \text{ Wb/m}^2$) at 15 Hz. The sample is 47 cm long, 5 mil diameter Nb-Ti. The voltage is always zero when $H = H_o$. The direction in time in which the oscilloscope trace proceeds is shown by an arrow in each picture. As the field approaches H_o there is always a voltage, as it reaches H_o the voltage goes to zero, then as the field decreases the voltage remains at zero

for a time roughly proportional to $\frac{I_c - I_s}{4f}$ (where $I_s =$ transport current) it then repeats the same pattern for the second half of the cycle. The pulses seen in certain sections of the trace are considered to be caused by flux jumps and will be discussed later.

These same pictures show that the maximum sample voltage (neglecting flux jumps) at constant frequency is proportional to I_s . Figure 15 shows V_s , the sample voltage, vs applied field at constant peak field and at a constant transport current at various field frequencies. It can be seen that the maximum voltage (neglecting the flux jumps) increases linearly with frequency. The maximum voltage (V_{max}) then, is proportional to fI_s . The total measured loss (helium boil-off) is the sum of the hysteresis loss and

$$\int V_s I_s dt.$$

Or:
$$\text{Loss} = \mu_o f \text{ Vol. } \oint M dH + f \oint V_s I_s dt$$

where Vol. = Volume of superconductor

f = frequency of the applied magnetic field

M = magnetization of the material, a function of both H and I

H = applied magnetic field

V_s = sample voltage

I_s = sample current

μ_o = constant

The magnetization and thus the hysteresis loss decrease as the transport current is increased.⁷ However, in all the superconductors studied thus far the total loss always increases as I_s approaches I_c . This situation can also be predicted from the Bean model and again the theoretical calculations are left to Appendix C.

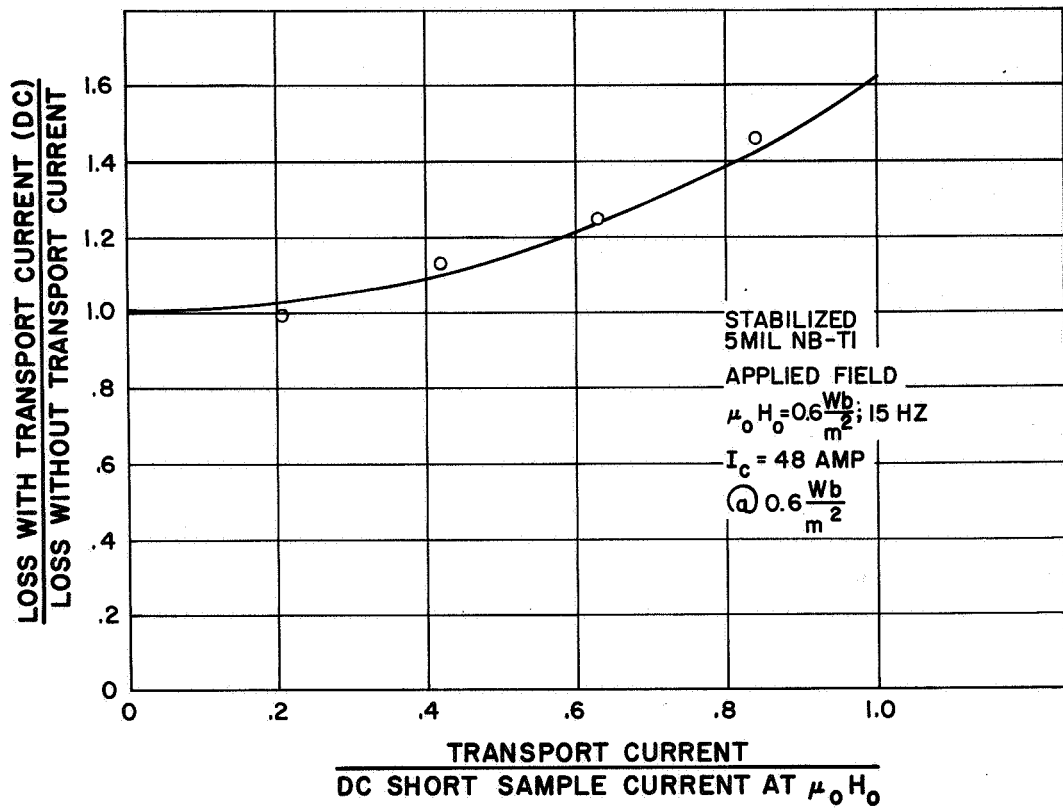


Fig. 13

Increase in Losses Due to Applied DC Transport Currents

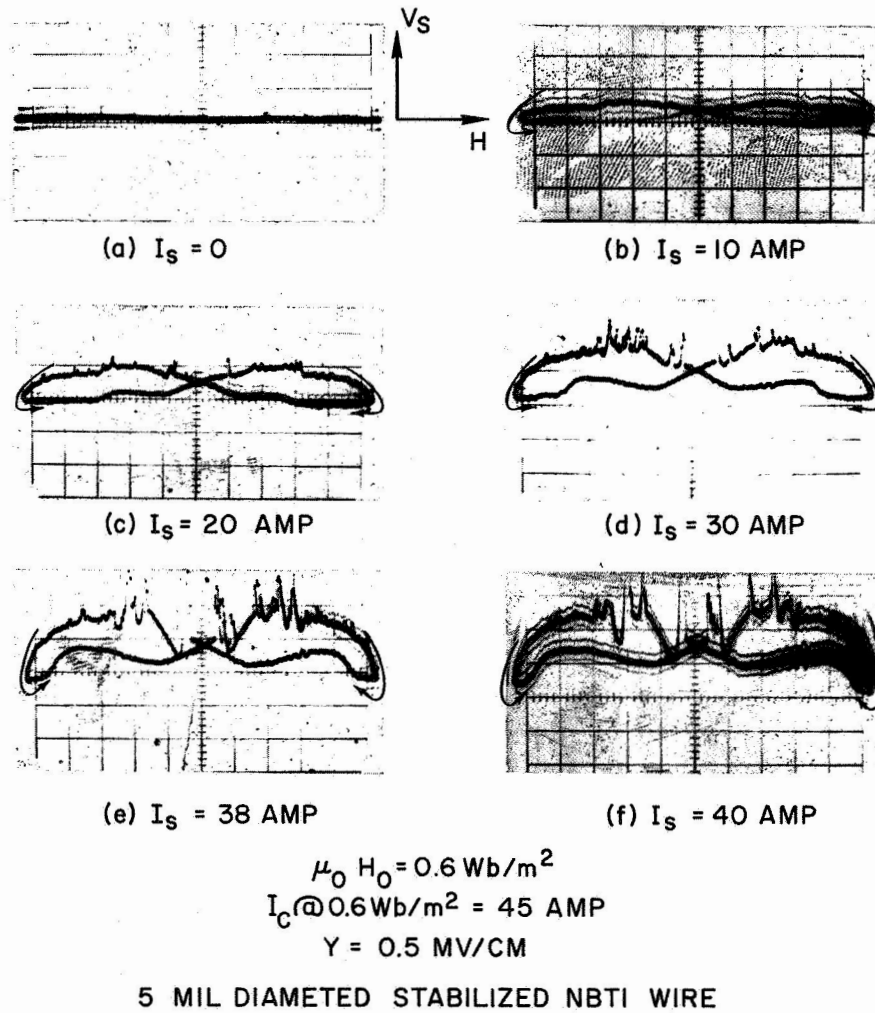
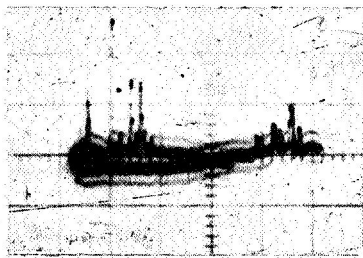
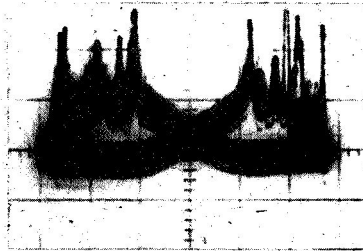


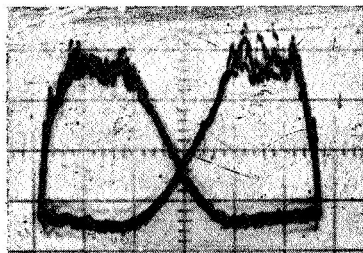
Fig. 14 Sample Voltage (V_S) vs Applied AC Magnetic Field at Various DC Transport Currents



(a) FREQ. = 15 HZ



(b) FREQ. = 30 HZ



(c) FREQ. = 60 HZ

5 MIL DIAMETER STABILIZED NBTI WIRE

$I_S = 30$ AMP-D.C.

$Y = 0.5$ MV/CM

$V_S = \text{ZERO}$ WHEN V_S IS A MINIMUM

$\mu_0 H_0 = 0.6$ Wb/m²

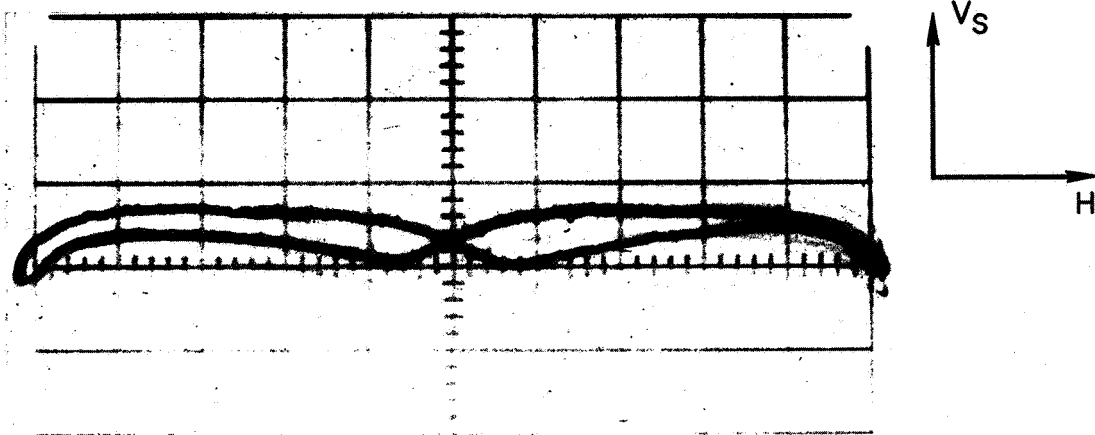
Fig. 15 Sample Voltage (V_S) vs Applied AC Magnetic Field at Various Frequencies

3) The observation of the flux jumps depends upon the wire diameter of the sample. Figure 16 shows V_s vs applied magnetic field for two stabilized Nb-Ti wires of different diameters (5 and 2.5 mil) with transport currents near their critical currents at the same peak applied field $H_0 = 0.6 \text{ Wb/m}^2$ H^* (5 mil) $\sim 0.5 \text{ Wb/m}^2$, H^* (2.5 mil) $\sim 0.25 \text{ Wb/m}^2$. The absence of flux jumps in the smaller diameter wire is easily noticed, yet J_c for both wires is approximately the same. In all the cases where flux jumping was observed, the applied magnetic field had just swept through zero (Figs. 14 and 15), which corresponds to the point of maximum magnetization. For a particular sample the flux jumps always occurred at the same place (with respect to H) if the sample was potted in epoxy to prevent motion of the wires. (See Fig. 14). The characteristic time for a flux jump to appear and disappear in Nb-Zr and Nb-Ti while carrying transport currents is several tenths of a millisecond. This time is lengthened by increasing the transport current. Flux jumps were never observed for the GE Nb-Sn ribbon even at currents approaching the short sample characteristic. However, the results are somewhat complicated by the fact that there is a large amount of Niobium and Copper in the GE tape and immediate conclusions cannot be drawn. As shown in Fig. 14 the maximum voltage created by flux jumps in stabilized 5 mil diameter Nb-Ti wire as a function of current is shown below in Table I.

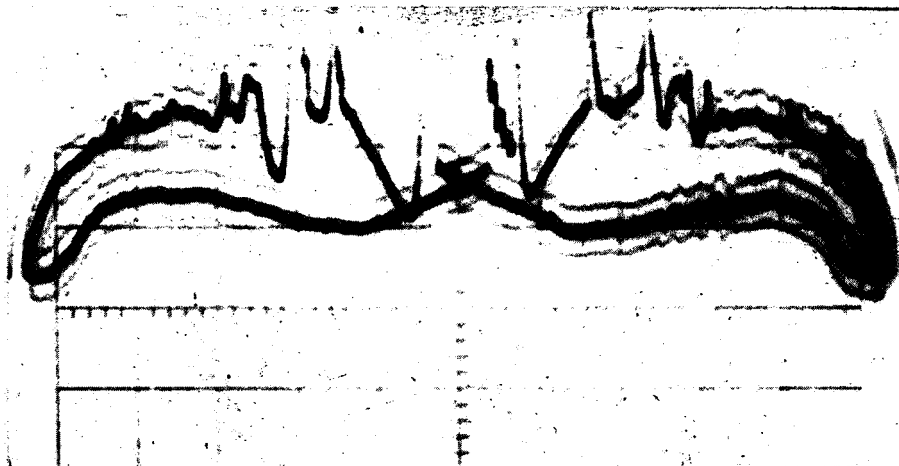
TABLE I

<u>I_s (DC)</u>	<u>Peak Voltage of Flux Jump</u>	<u>Max. Length</u>
10 amp	0.1 MV	.4 cm
20 amp	0.25 MV	.5 cm
30 amp	0.7 MV	.9 cm
40 amp	1.4 MV	1.3 cm

If it is assumed that during a flux jump, a section of the superconductor exhibits its normal resistivity, then the voltage generated is due to the transport current flowing in the copper used to stabilize the superconductor. This is so because the normal resistance of the superconductor is approximately 5×10^3 times larger than that of copper. Thus the peak voltage observed is just the resistance per unit length of the copper times the maximum length of the normal region times the transport current. The maximum length attained by the normal spot is given in the last column of the above table. The initial size of the normal spot, however, cannot be determined from the data taken, but it is less than 0.1 cm.



(a) 2.5 MIL DIA. $I_c \approx 11$ AMP @ 0.6 Wb/m^2
NO FLUX JUMPS EVIDENT



(b) 5 MIL DIA $I_c \approx 48$ AMP @ 0.6 Wb/m^2
FLUX JUMPS CLEARLY EVIDENT

$$\mu_0 H_0 = 0.6 \text{ Wb/m}^2$$

STABILIZED NBTI WIRES. (a) 2.5 MIL DIA $I_s \approx I_c$, (b) 5.0 MIL DIA $I_s \approx I_c$. FIELD FREQUENCY = 15 HZ. $\gamma = 0.5 \text{ MV/CM}$

Fig. 16 Effect of Wire Diameter on Flux Jumping

D. Losses Due to AC Transport Current and AC Fields

Alternating currents of the same frequency as the magnetic field were also applied to the sample. Several different phase angles between the magnetic field and the current were established. The result was that the total loss always increased. This increase is about 50% when I_s approaches I_c . The exponent of H_0 determined in the second experiment, where only an externally applied AC field is present, is approximately 3.2 whereas in the first experiment, where both AC currents and the self AC field is present, the exponent is 3.7. This higher exponent is due to interaction between the transport current and the self field it creates in the superconductor.

REFERENCES

1. Iwasa, Y. and Montgomery, D. Bruce, "Flux Creep as a Dominant Source of Degradation in Superconducting Solenoids," Appl. Phys. Letts. 7, 9, 1965.
2. Kantrowitz, A.R. and Stekly, Z. J. J., "A New Principle for the Construction of Stabilized Superconducting Coils," Appl. Phys. Letts. 6, 56, 1965.
3. Weisseman, Boatner, Low, "Alternating Current Power Losses in Superconducting Nb-Zr Alloys," J. Appl. Phys. 9, 35, 1964.
4. Bogner, G. and Heinzl, W., "Wechselstrommessungen an Harten Supraleitern," "Solid-State Electronics," Vol. 7, 1964.
5. Pech, T., Duflot, J. P., and Fournet, G., "Comparative Measurements of 50 C/S Losses in Superconductors," Phys. Letts. Vol. 16 No. 3, 1965.
6. Bean et al, "A Research Investigation of the Factors that Effect the Superconducting Properties of Materials," G. E. -AFML-TR-65-431, March 1966.
7. LaBlanc, M. A. R., Phys. Rev. Letts. 11, 149 (1963).
8. Kruger, P. and Oswald, B., "Homogeneity Investigations on Superconducting Wires and Cables," Institut für Plasmaphysik IPP 4/31, April 1966.
9. Kim, Y. B. et al, Phys. Rev. Letts. 9, 306 (1962); Phys. Rev. 129, 528 (1963).

APPENDIX A

LOSSES DUE TO AC TRANSPORT CURRENTS

A system was designed and built to drive up to 60 amp rms through a superconducting sample at frequencies from 50 Hz to 2000 Hz. A schematic of the system is shown in Fig. A-1. The power dissipated is calculated by measuring the sample voltage (V_s), the sample current (I_s) and the phase angle between them. A wave analyzer is used to study the harmonics in the sample voltage. The sample current is constrained to be of a single frequency by the relatively large impedance of the circuit as compared to the sample.

I_s is measured by measuring the voltage across a frequency calibrated shunt. V_s is measured by the wave analyzer after it has been amplified by a known factor. The phase angle is measured by monitoring the DC output of a Hall Effect Multiplier, which multiplies aI_s and bV_s , where a and b are known constants.

For the Hall Multiplier:

$$V \text{ (output)} = K I_H V_H$$

where

$$K = \text{constant (known)}$$

$$I_H = \text{Hall input current}$$

$$V_H = \text{Hall input voltage}$$

$I_H = bV_s$, $V_H = aI_s$ where a and b are constants determined by the system elements.

$$V \text{ (output)} = abKI_s V_s$$

$$\text{Now } I_s = I_1 \sin wt$$

$$\text{and } V_s = \sum_{N=1}^{\infty} V_N \sin (N wt + \theta_N)$$

where w = angular frequency

$$\theta_N = \text{phase angle between } (N - 1)^{\text{th}} \text{ harmonic and } I_s$$

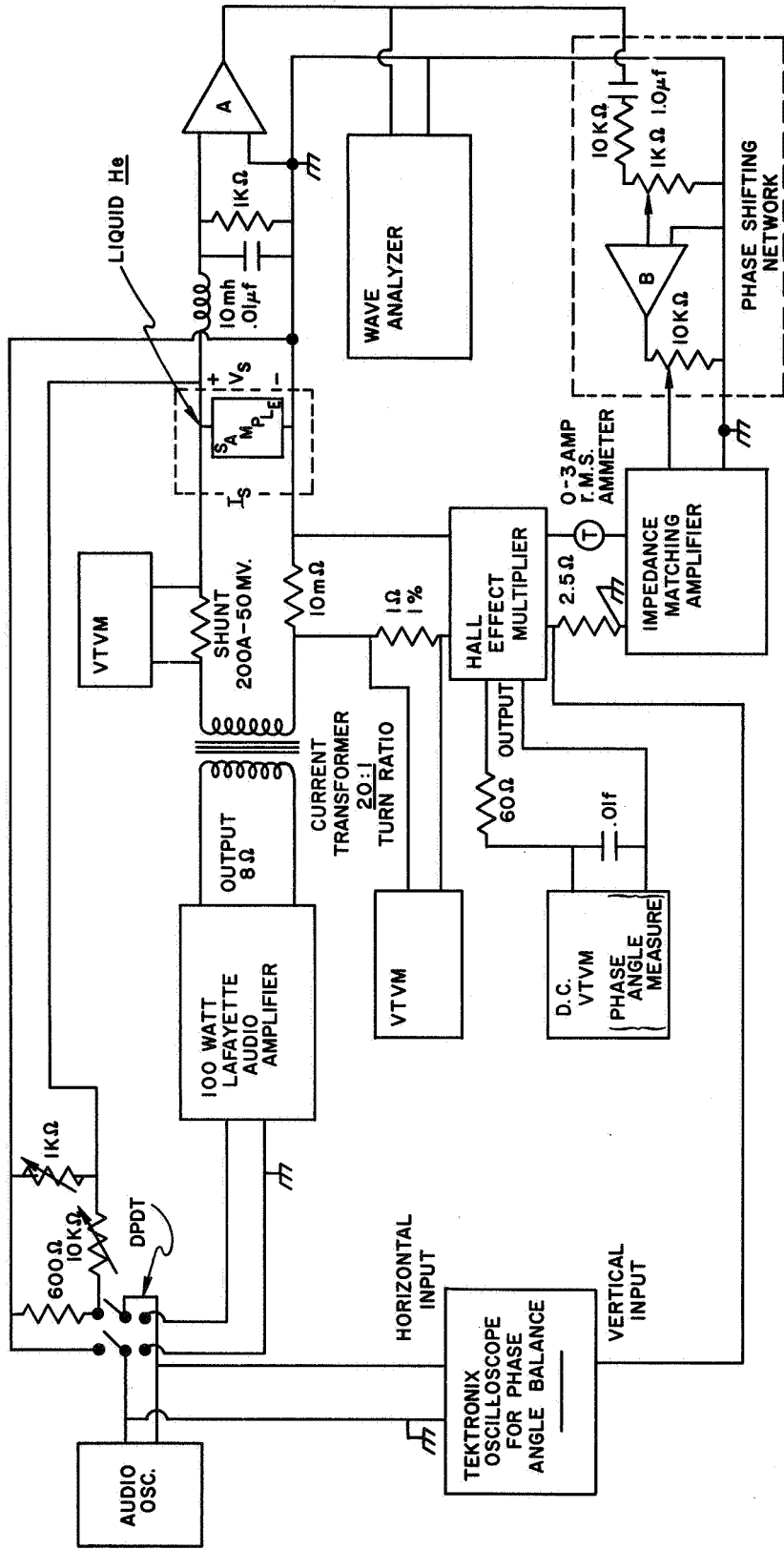


Fig. A-1 Experimental Setup for Measuring Losses With Applied AC Currents

$$V \text{ (output)} = a b k I_1 \left[V_1 \sin^2 \omega t \cos \theta_1 + V_1 \cos \omega t \sin \omega t \sin \theta_1 + \sum_{N=2}^{\infty} V_N \sin \omega t \cdot \sin (N \omega t + \theta_N) \right]$$

$$V \text{ (output)} = a b k I_1 \left[V_1 \frac{\cos \theta_1}{2} - V_1 \frac{\cos 2 \omega t}{2} \cdot \cos \theta_1 + V_1 \cos \omega t \sin \omega t \sin \theta_1 + \sum_{N=2}^{\infty} V_N \sin (N \omega t + \theta_N) \cdot \sin \omega t \right]$$

The DC term in the output is

$$V \text{ (output DC)} = \frac{k (a I_1) (b V_1) \cos \theta_1}{2}$$

$$\text{Thus } \cos \theta_1 = \frac{2 V \text{ (DC)}}{K V_H I_H}$$

$$\text{and thus Power loss} = \frac{I_1 V_1}{2} \cos \theta_1 \text{ (watts)} = I_1 \text{ (rms)} V_1 \text{ (rms)} \cos \theta_1$$

Measurements of the harmonics in V_s reveal that only odd harmonics are present. These measurements are summarized in Fig. A-2. At constant input current, the voltage of the harmonics is proportional to frequency.

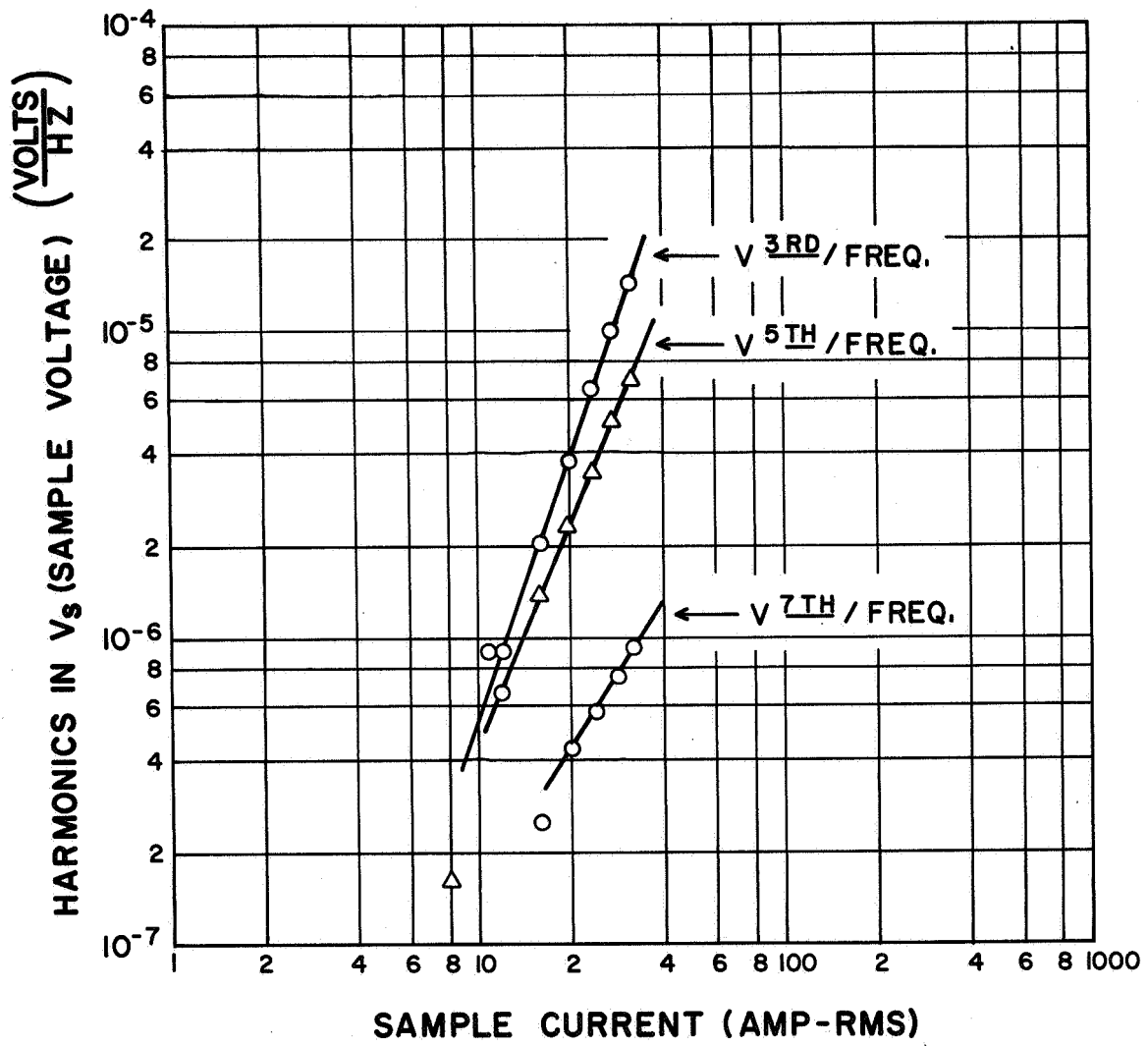


Fig. A-2 Sample Voltage Harmonics vs Sample Current in Nb-Zr Wire

APPENDIX B

APPARATUS FOR APPLYING AC FIELDS

A magnet was made from iron-silicon strip and designed to be powered from a 1.2 kVA motor-generator modified to run at speeds from 300 rpm to 7000 rpm. The test setup is diagrammed in Fig. B-1. The losses are calculated by measuring the helium boil-off from the sample alone. In order to do this, a phenolic boil-off "jacket", which had small vents in the side to admit liquid helium and a stainless steel tube at the top to channel the gas flow, was made to place around the sample. The magnet and boil-off jacket are pictured in Fig. B-2. The magnet was calibrated and the field as a function of position was measured. The field produced in the gap is $0.1 \text{ Wb/m}^2\text{-Amp}$ (magnet coil current). The peak field produced in the gap at saturation of the iron is 6 kilogauss; thus, the maximum operating field is set at about 0.6 Wb/m^2 . An integrating flow meter was used to measure the boil-off and losses as low as a milliwatt could be detected. The sample was wound onto a phenolic form .350" in diameter and .230" long and held in place in the boil-off jacket by a phenolic pin. One pickup coil made from approximately 10 to 12 turns of #35 copper wire was under the sample and another over the sample.

The magnetization of the sample is measured by two pickup coils concentric with the cylindrical coil sample. The applied field is axial so, neglecting end effects, the field in the superconductor (H_{int}) is the same as the applied field (H_{ext}). Thus let

(MKS units used) $N_1, r_1 =$ turns, radius of inner pickup coil

$N_2, r_2 =$ turns, radius of outer pickup coil

$$H_{\text{ext}} = H_0 \sin \omega t, \text{ and } B = \mu_0 (H + M)$$

then

$$V_1 = \mu_0 N_1 \pi r_1^2 H_0 \omega \cos \omega t \text{ (inner coil)}$$

and

$$V_2 = \mu_0 N_2 \left[\pi r_2^2 H_0 \omega \cos \omega t + \pi (r_2^2 - r_1^2) \frac{dM}{dt} \right] \text{ (outer coil)}$$

where

$M =$ magnetization of the superconductor.

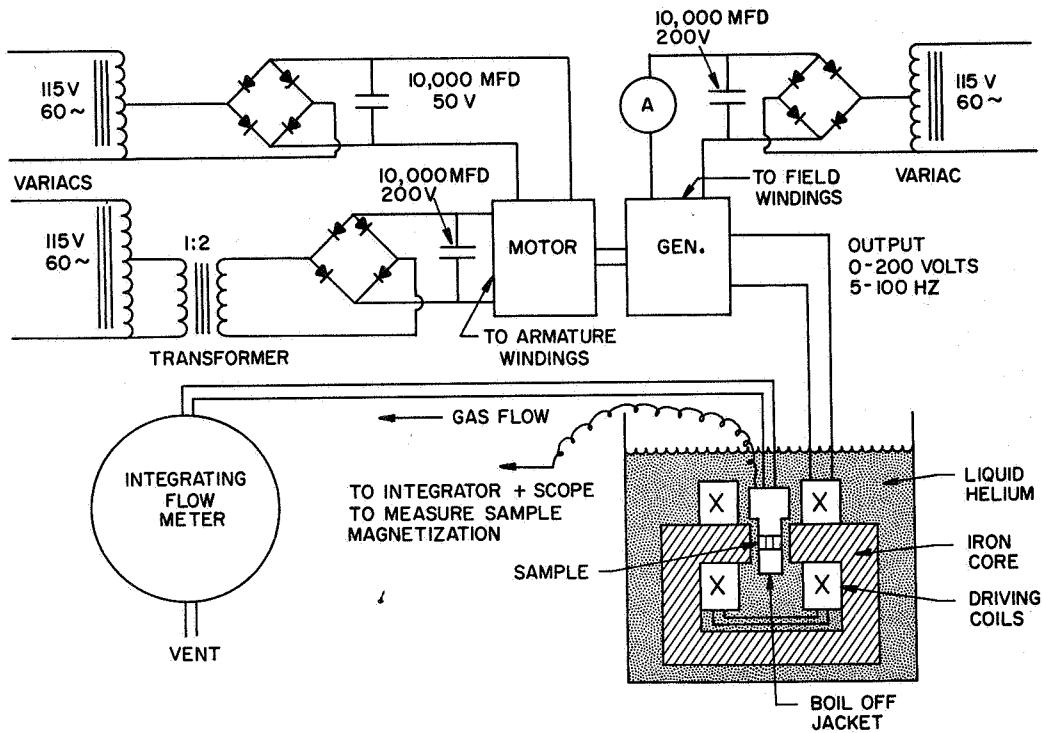


Fig. B-1 Experimental Setup for Measuring Losses with Applied AC Magnetic Fields

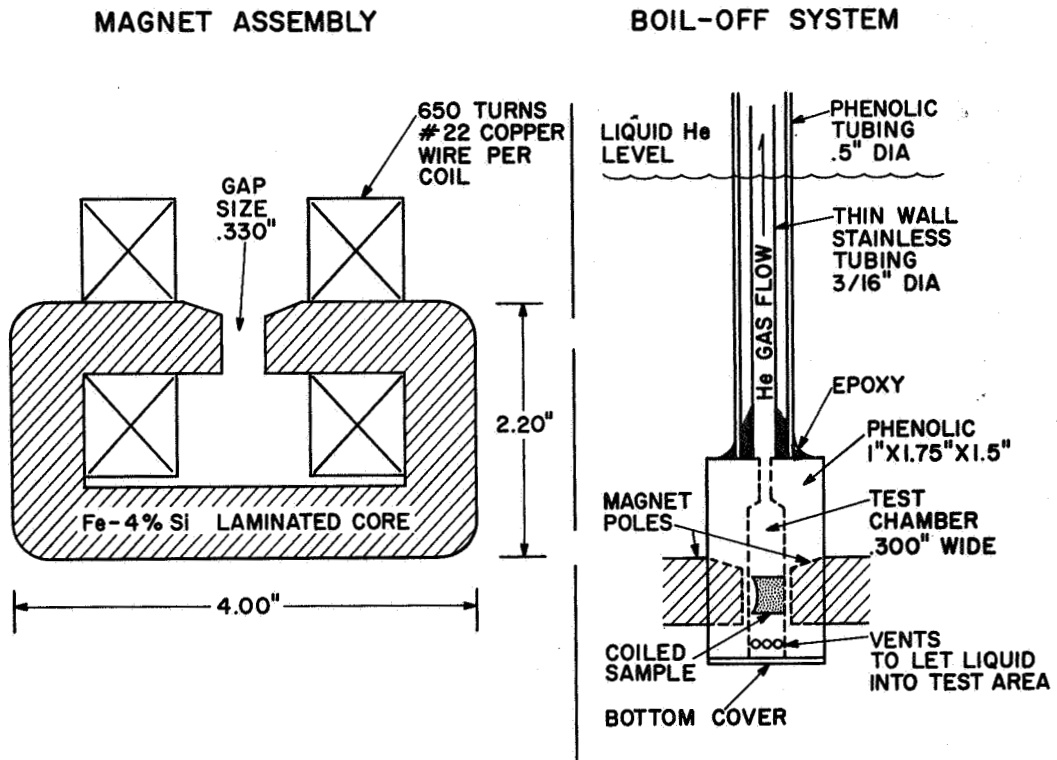


Fig. B-2 Details of Sample Holder and Magnet

thus

$$V_o = V_2 - V_1 = \mu_o \pi (w H_o [N_2 r_2^2 - N_1 r_1^2] \cos wt + N_2 (r_2^2 - r_1^2) \frac{dM}{dt})$$

and if

$$N_2 r_2^2 - N_1 r_1^2 = 0$$

then

$$V_o = \mu_o \pi N_2 (r_2^2 - r_1^2) \frac{dM}{dt}$$

and

$$\frac{1}{\mu_o \pi N_2 (r_2^2 - r_1^2)} \int V_o dt = M$$

The hysteresis loss is given by: loss per cycle = $\mu_o V \oint MdH$
 where

V = volume of superconductor

$$\mu_o = 4\pi \times 10^{-7}$$

To obtain the hysteresis loop V_o is integrated and plotted on the y axis of an oscilloscope while the x axis is driven by $x = x_o \sin wt = c H_o \sin wt$. In the experiment, $N_2 \neq N_1 r_1^2 / r_2^2$ but is slightly different, so part of the variable plotted on the y axis was H.

Thus the area of the experimental loop was proportional to

$$\oint VdH = c_1 \oint HdH + C_2 \oint MdH = C_2 \oint MdH, \text{ since } \oint HdH = 0$$

That is to say, even though the trace given is not the exact hysteresis curve, the area enclosed still represents the hysteresis loss. Some experimental traces are shown in Fig. VI-7.

APPENDIX C

LOSS CALCULATION USING THE BEAN MODEL

The critical state model of Type II superconductors as proposed by Bean⁶ has been successful in explaining all the AC effects observed. This model is based on two assumptions:

- 1) If an electric field exists at a point in the superconductor, a local current is caused to flow, its current density being J_C . This current persists even if the electric field is reduced to zero. It may be reversed, however, if the electric field is reversed — but again persists when the electric field is reduced to zero.
- 2) There is a given J_C versus H (applied magnetic field) relationship given for the material.

With these assumptions and Maxwell's Equations, one can theoretically calculate the loss in the superconductor when an AC magnetic field is applied. For simplicity in calculation Bean⁶ assumes that $J_C = \text{constant}$ (independent of H). An "outside limit" is put on the J_C versus H characteristic as measured by Kim et al.,⁹ $J_C H = \text{constant}$. Since the actual J_C versus H characteristic falls between these two limits it is expected that the losses measured ought to fall between these two limits. These limits are called the Bean and Kim limits respectively. The methods of calculation of losses used by Bean have been to:

- 1) Calculate $E \cdot J$ over the superconductor volume
- 2) Integrate the Poynting vector over the surface of the superconductor.
- 3) Calculate the hysteresis loss - used when no transport currents are flowing.

Several calculations follow, using the Bean assumption, (J_C independent of H) which derive the losses obtained in an infinite superconducting slab subjected to an AC magnetic field. The results are later shown to apply to the experimental results.

A. Losses Without Transport Current

The calculations are done for an infinite slab, thickness $2a$. The geometry is shown in Fig. C-1(a).

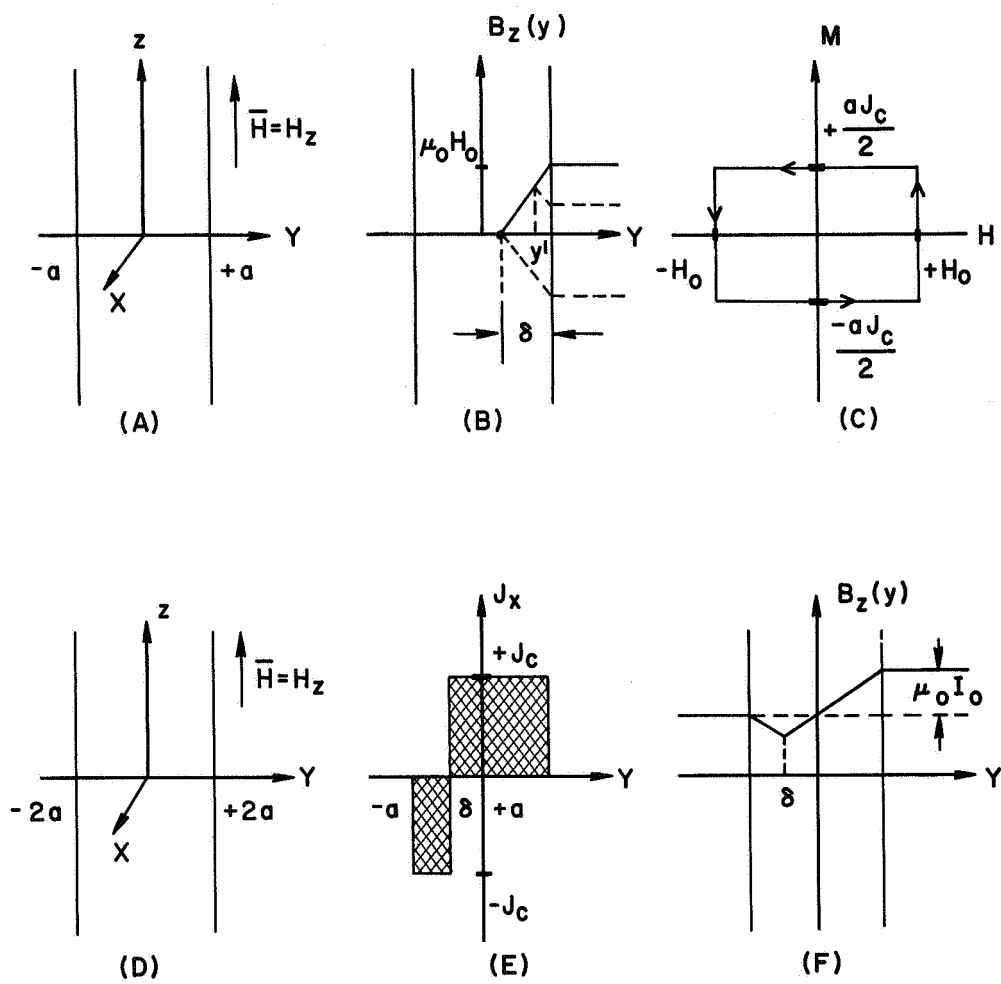


Fig. C-1 Magnetic Flux Penetration at Different Applied Magnetic Fields

Given: $H_z = H_0 \sin \omega t$

The magnetic field is "turned on" at $t = 0$

Maxwell's Equations: (MKS system)

$$1) \nabla \times E = -\frac{\partial B}{\partial t} \quad 2) \nabla \times B = \mu_0 J \text{ (neglecting displacement currents)}$$

$$\text{and } 3) B = \mu_0(H + M)$$

There are no currents flowing in the sample for $t \leq 0$.

where: H = magnetic field intensity amp-turns/m
 B = magnetic flux density weber/m²
 E = electric field intensity volts/m
 J = current density amps/m²
 M = magnetization of material amp-turns/m
 μ_0 = constant ($4\pi \times 10^{-7}$) weber-amp/m²

As H increases from zero an electric field is generated at the surface of the conductor (since $\nabla \times E = -\mu_0 \frac{\partial H}{\partial t}$ at the surface). From symmetry the electric fields at the surfaces are equal but in opposite directions. The currents caused by these fields tend to oppose any change in magnetic flux density B , in the material (Lenz's Law). Thus B "decays" from the surface into the superconductor. If H_0 is large enough, B will penetrate the whole conductor. B_z varies only with the coordinate y and time t and Eq. 2 gives

$$4) \quad \frac{\partial B_z}{\partial y} = \mu_0 J_x; \quad |J_x| = J_c$$

Thus the slope of B_z is constant in magnitude. Figure C-2 shows B_z as a function of the coordinate y at different values of H . The progression in time of the field penetration is from a to g ($0 < t < \frac{5\pi}{2\omega}$) and then repeats cyclicly from c to g for all t .

Loss Calculations:

1) Definition of H^* : H^* is the minimum field necessary to make B penetrate fully into the superconductor. Thus H^* may be calculated from (4)

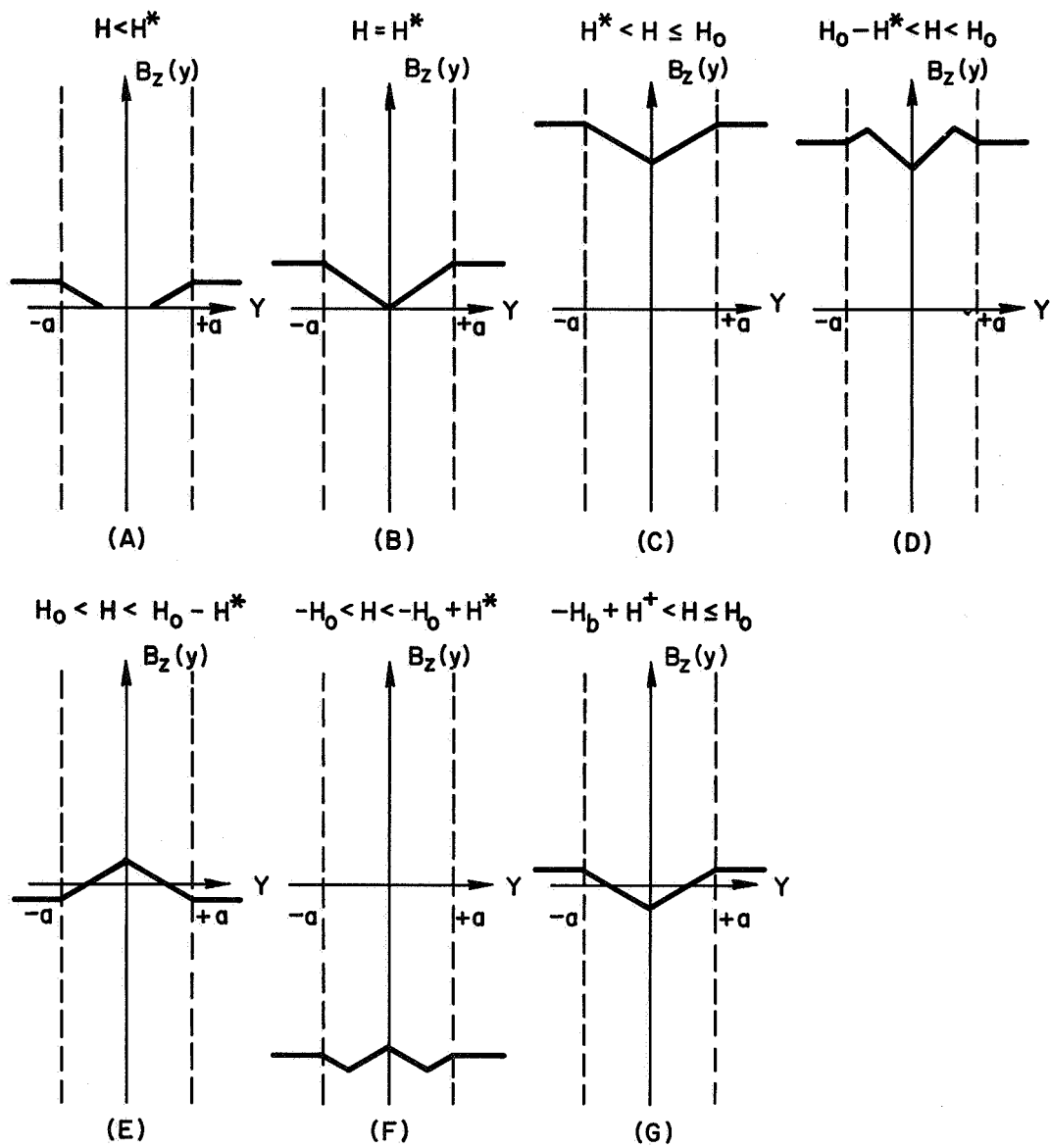


Fig. C-2 Figures Used for Calculations in Appendix C

$$\int_{B_z(0)}^{B_z(a)} \partial B_z = \mu_0 J_c \int_0^a dy \quad B_z(0) = 0$$

$$\therefore B_z(a) = \mu_0 J_c a, \quad H^* = \frac{B_z(a)}{\mu_0} = J_c a$$

2) Case #1 $H_0 < H^*$, then B, E do not fully penetrate the superconductor, and the loss per unit surface area is independent of the thickness (2a). The net energy input per unit surface area of superconductor per cycle is given by the time integral of the Poynting vector over that surface per cycle.

Now $S(\text{Poynting vector}) = \vec{E} \times \vec{H} = -E_x H_z$. H_z is given. To compute E calculate $\dot{\phi}$ (time derivative of the magnetic flux in the sample). $B_z(y)$ as a function of time is given by:

$$(5) B_z(y) = \mu_0 H_0 - \mu_0 J_c (a - y), \quad a - \delta < y < y'$$

$$(6) B_z(y) = \mu_0 H + \mu_0 J_c (a - y), \quad y' < y < a$$

$$\text{and } y' = a - \frac{H_0(1 - \sin \omega t)}{2J_c} \text{ when } H \text{ is decreasing from } +H_0 \text{ to } -H_0.$$

where: δ is the maximum penetration depth of B and y' = dummy variable

$$\delta = \frac{H_0}{J_c}$$

An example of the geometry and field configuration is shown in Fig. C-1(b).

and:

$$E_x(a) = \frac{\partial}{\partial t} \left(\int_{a-\delta}^{y'} B_z(y) dy + \int_{y'}^a B_z(y) dy \right)$$

$$E_x(a) = \frac{\mu_0 H_0^2 \omega}{2J_c} (1 - \sin \omega t) \cos \omega t$$

$$\text{and } S_y(a) = - \frac{\mu_0 H_0^3 \omega}{y J_c} (1 - \sin \omega t) \cos \omega t \sin \omega t$$

for the period of time in which H is decreasing from H_0 to $-H_0$ (the first half of a cycle). $S_y(a)$ will be equal in magnitude and direction when H is increasing from $-H_0$ to H_0 (the other half of the cycle).

The energy loss per cycle is the time integral of S_y per cycle:

$$\text{Energy} = 2 \times \frac{\mu_0 H_0^3}{2J_c} \int_{\pi/2\omega}^{3\pi/2\omega} \omega(1 - \sin \omega t) \cos \omega t \sin \omega t \, dt.$$

$$\text{Energy loss} \left(\frac{\text{Joules}}{\text{cycle} - \text{m}^2 \text{ (surface area)}} \right) = \frac{2}{3} \frac{\mu_0 H_0^3}{J_c}$$

For $H_0 < H^*$ the power dissipated under AC conditions:

- 1) increases linearly with frequency
- 2) increases as H_0^3
- 3) varies inversely as J_c

If we had assumed that $J_c H = C(T)$ (Kim's model, where $C(T)$ is a decreasing function of temperature) we would have found:

$$\text{Loss} \propto \frac{H_0^4}{C(T)}, \quad H_0 < H^*$$

Thus, since $C(T)$ decreases as temperature increases, in this regime the loss would increase as temperature increased. This is the reason for the increase in loss in Fig. 3. This increase has been observed by others.³

3) Case #2 $H_0 \gg H^*$. Neglecting the small amount of time when $H_0 - H^* < |H| < H_0$ we have:

$$B_z(y) = B_z(a) \pm \mu_0 J_c (a - y), \quad 0 < y < a$$

$$B_z(y) = B_z(a) \pm \mu_0 J_c (a + y), \quad -a < y < 0$$

The upper sign before μ_0 applies when H is decreasing, the lower sign when H is increasing. The volume average magnetization is defined as:

$$\frac{\bar{B}}{\mu_0} - H = \bar{M} = \frac{1}{2a\mu_0} \int_{-a}^a B_z(y) dy - H$$

$$\therefore \bar{M} = \pm \frac{J_c a}{2} \quad \begin{array}{l} + H \text{ is decreasing} \\ - H \text{ is increasing} \end{array}$$

The magnetization curve is shown in Fig. C-1(c), and the energy loss per cycle per m^3 is $\mu_0 \oint \text{MdH}$.

$$\text{Energy loss} \quad \frac{\text{Joules}}{\text{Cycle} \cdot m^3} = 2\mu_0 a J_c H_0$$

For $H_0 \gg H^*$ the power dissipated under AC conditions:

- 1) again increases linearly with frequency
- 2) increases as H_0
- 3) increases linearly with J_c

The loss calculated is the same if we compute $\vec{E} \cdot \vec{J}$ over the superconductor volume per cycle - as it should be.

If we had assumed a modified Kim's model $J_c(H+H_1) = C(T)$ we would have found

$$\text{Loss} \propto a C(T) \ln \left(\frac{H_0 + H_1}{H_1} \right), \quad H_0 \gg H^*$$

where H_1 is a constant, characteristic of the material and if $H_1 \ll H_0$ then:

$$\text{Loss} \propto a C(T) \ln H_0$$

Thus, since $C(T)$ decreases with increasing temperature, the losses decrease, in this case, with increasing temperature. The transition from a loss dependence of H_0^3 to H_0^4 is quite rapid as seen in the experiment.

4) The Effect of Stabilization - Eddy Current Losses

In order to stabilize the superconductor, it is necessary to heavily shunt the superconductor with a high conductivity material. Thus in AC

fields there will be an eddy current loss in this conductor. The stabilized samples themselves were shunted with copper on both sides of the superconductor and the total thickness is twice that of the superconductor. Thus to approximately compare the eddy current losses to the superconducting losses take a slab of copper (thickness $4a$) and calculate the losses in it. These losses should be much less than the superconductor losses in the range of frequency and field values of the experiment. If the half-thickness of the copper is smaller than the skin depth of the AC magnetic field then we can assume $H = H_0 \sin \omega t$ throughout the material. In the experiment the maximum thickness of the sample is 10 mils, the skin depth of copper at 4.2°K , 100 Hz is about 20 mils; therefore, the assumption is well justified. The eddy current loss is: (See Fig. C-1(d) for geometry).

$$\left| E_x \right| = \mu_0 H_0 y \omega \cos \omega t \quad -2a < y < 2a$$

Loss per unit volume is:

$$L = \frac{\ell h}{4a \ell k} \cdot 2 \int_0^{2a} \sigma E_x^2 dy$$

where: ℓ , h are dimensions in x , z direction,

σ is the material conductivity

$$L = \sigma (\mu_0 H_0 \omega \cos \omega t)^2 \frac{(2a)^2}{3}$$

The time average loss is

$$L \left(\frac{\text{Watts}}{\text{M}^3} \right) = \frac{\sigma \mu_0^2 H_0^2 \omega^2 (2a)^2}{6}$$

Now the superconductor loss should be much greater than the eddy current loss.

$$\omega / 2\pi \cdot 2 \mu_0 J_c a \gg \frac{\sigma \mu_0^2 H_0^2 \omega^2 (2a)^2}{6}$$

or $J_c \gg \sigma \mu_0 H_0 \omega \frac{4a}{6} \cdot \pi$ when $H_0 \gg H^*$. In the experiment:

$$\mu_0 H_0 (\text{max}) = .6 \omega / \text{m}^2$$

$$\omega (\text{max}) = 314 \text{ sec}^{-1} @ .6 \omega / \text{m}^2$$

$$a (\text{max}) = 6.4 \times 10^{-5} \text{ m}$$

$$\sigma = 9 \times 10^9 \text{ mho/m}$$

Thus for the superconductor loss to be greater than the eddy current loss

$$J_c > 2.4 \times 10^4 \text{ amp/cm}^2$$

The actual J_c for the stabilized wires of this size is about $6 \times 10^5 \text{ amp/cm}^2$. Thus the eddy current loss may be ignored in this experiment when $H_o > H^*$. However, at some field $H_o < H^*$ the eddy current loss will dominate since: superconductor loss $\propto H_o^3$ and Eddy loss $\propto H_o^2$

$$\frac{\text{Eddy loss}}{\text{Superconductor loss}} \propto \frac{1}{H_o}$$

For small enough H_o this ratio of losses will become larger than 1.

B. Losses with DC Transport Currents

If transport currents are carried by the sample the magnetization decreases - yet the total loss is observed to increase. For an initial case let us assume that the transport current is DC ($0 < I_o < I_c$) and $H_o \gg H^*$. At some $|H_z| < H_o - H^*$ apply a current I_o per unit z , then the current distribution in the slab for increasing H is shown in Fig. C-1(e).

The transport current is:

$$|I_o| = \left| \int_{-a}^a J_x dy \right| = 2 |\delta| J_c \text{ or } \delta = -\frac{I_o}{I_c} a$$

Now on opposite sides of δ the electric fields must be in opposite directions (for J to be in opposite directions). Thus:

$$E_x(\delta+) + E_x(\delta-) = \frac{\partial B}{\partial t} \Delta \delta; \text{ and as } \Delta \delta$$

goes to zero:

$$E_x(\delta+) + E(\delta-) = 0 = E(\delta+) = E(\delta-)$$

Thus at δ the electric field must go to zero. Now E_x versus y is found from Eq. 1. The magnetic flux distribution in the superconductor is shown in Fig. C-1(f).

$$B_z(y) = \mu_o H - \frac{\mu_o I_o}{2} - \mu_o J_c (a+y) \quad -a < y < \delta$$

$$B_z(y) = \mu_o H + \frac{\mu_o I_o}{2} + \mu_o J_c (a-y) \quad \delta < y < a$$

δ is fixed in time

Thus

$$E_x(y) = \int_{\delta}^y \frac{\partial B_z(y)}{\partial t} dy \quad \delta < y < a$$

$$E_x(y) = - \int_y^{\delta} \frac{\partial B_z(y)}{\partial t} dy \quad -a < y < \delta$$

$$\therefore E_x(y) = \mu_o H_o \omega (y - \delta) \cos \omega t \quad -a < y < a$$

This is for the half cycle where H is increasing - when H is decreasing the situation is symmetric. That is, the loss is the same in the decreasing half of the cycle as it is in the increasing half. Neglecting the small period of time when $H - H^* < |H| < H_o$ the average energy loss per unit volume is given by:

$$\text{Energy loss} = \frac{1}{2a} \iint E_x J_x dy dt$$

$$\text{Energy loss} \left(\frac{\text{Joules}}{\text{Cycle} - M^3} \right) = \frac{2 \times 2\mu_o H_o J_c}{2a} \left[\int_{\delta}^a (y - \delta) dy - \int_{-a}^{\delta} (y - \delta) dy \right]$$

$$= \frac{2\mu_o H_o J_c}{a} (a^2 + \delta^2)$$

or equivalently

$$= 2\mu_o H_o J_c a \left[1 + \left(\frac{I_o}{I_c} \right)^2 \right] \frac{\text{Joules}}{\text{Cycle} - M^3}$$

The ratio of the loss with transport current to the loss without transport current is

$$\frac{\text{Loss with } I_o}{\text{Loss without } I_o} = 1 + \left(\frac{I_o}{I_c} \right)^2 \quad (\text{DC Currents})$$

This model gives fairly accurate results for this case (see Fig. 13) even though the assumption that $J_c = \text{constant}$ (independent of H) is only roughly correct.

C. Losses With AC Transport Currents

The magnetic flux distribution is the same as the DC case (Fig. C-1(f)), but now both δ and I are a function of time.

Assume:

$$H = H_0 \sin \omega t$$

$$I = I_0 \sin \omega t$$

H is increasing from $-H_0$ to H_0

Again

$$B_z(y) = \mu_0 H + \frac{\mu_0 I}{2} - \mu_0 J_c (a - y) \quad \delta < y < a$$

$$B_z(y) = \mu_0 H - \frac{\mu_0 I}{2} - \mu_0 J_c (a + y) \quad -a < y < \delta$$

$$\delta = -\frac{I_0 a}{I_c} \sin \omega t$$

and remembering that $E_x(\delta)$ must equal zero:

$$E_x(y_0) = \frac{\partial}{\partial t} \int_{\delta}^{y_0} \left[\mu_0 H + \frac{\mu_0 I}{2} - \mu_0 J_c (a - y) \right] dy \quad \delta < y < a$$

$$E_x(y_0) = -\frac{\partial}{\partial t} \int_{y_0}^{\delta} \left[\mu_0 H - \frac{\mu_0 I}{2} - \mu_0 J_c (a + y) \right] dy \quad -a < y < \delta$$

The power dissipation per unit volume is:

$$P = \frac{J_c}{2a} \left[\int_{\delta}^a E_x(y_0) dy - \int_{-a}^{\delta} E_x(y_0) dy \right]$$

and the energy loss per cycle per M^3 is:

$$\text{Loss} \left(\frac{\text{Joules}}{\text{Cycle} - M^3} \right) = 2x \int_{-\pi/2\omega}^{\pi/2\omega} P dt$$

Thus the energy loss is:

$$2 \mu_0 J_c H_o a \left(1 + \left(\frac{I_o}{I_c} \right)^2 \right) \frac{\text{Joules}}{\text{Cycle} - M^3}$$

The same as the DC case! That this could be so evident from the following argument:

1) In the DC case $E_x(y) \propto \frac{\partial}{\partial t} (B \cdot A) = \dot{B}A$ where A is the area from δ to some point y.

2) In the AC case $E_x(y) \propto \frac{\partial}{\partial t} (B \cdot A) = \dot{B}A + B\dot{A}$, again where A is the area from δ to y - because $\delta = f(t)$

Thus in the AC case the average rms electric field is higher but the average rms current is lower - the net effect is that the loss remains the same. This seems to be contrary to a calculation by Buchhold⁶ which finds the AC loss proportional to

$$1 + \frac{1}{3} \left(\frac{I_o}{I_c} \right)^2$$

D. Applicability of Theoretical Results to Experiment

The samples are made from single layer, open-circuited Bifilar solenoids. The applied field is axial and exhibits some fringing in the magnet gap. Thus the magnetic field varies somewhat both in direction and magnitude from place to place in the sample. As a rough approximation, however, the sample may be assumed to be a long open circuited cylinder with a purely axial field. For points sufficiently near the cylinder surface, if the thickness is much less than the diameter, the surface looks like an infinite plane sheet. In the experiment the diameter of the sample is ≥ 40 times its thickness, so we expect the results of the theory for an infinite slab to hold in the experiment, at least in the first approximation.